Effects of RF Impairments in Communications Over Cascaded Fading Channels

Alexandros-Apostolos A. Boulogeorgos, *Student Member, IEEE*, Paschalis C. Sofotasios, *Member, IEEE*, Bassant Selim, *Student Member, IEEE*, Sami Muhaidat, *Senior Member, IEEE*, George K. Karagiannidis, *Fellow, IEEE*, and Mikko Valkama, *Senior Member, IEEE*

***Abstract*—Direct-conversion architectures can offer highly integrated low-cost hardware solutions to communication transceivers. However, it has been demonstrated that radio frequency (RF) impairments such as amplifier nonlinearities, phase noise, and in-phase/quadrature-phase imbalances (IQI) can lead to severe degradation of the performance of such systems. Motivated by this, the present work is devoted to the quantification and evaluation of the effects of RF IQI on wireless communications in the context of cascaded fading channels for both single-carrier and multicarrier systems. To this end, closed-form expressions are first derived for the outage probability (OP) over N^* Nakagami-m channels for the cases of ideal transmitter (TX) and receiver (RX), ideal TX and IQI RX, IQI TX and ideal RX, and joint TX/RX IQI. The offered expressions, along with several deduced corresponding special cases, are subsequently employed in vehicle-to-vehicle (V2V) communications to justify their importance and practical usefulness in the context of emerging communication systems. The offered analytic results are corroborated by extensive comparisons with respective results from computer simulations. It is shown that considering non-ideal RF front-ends at the TX and/or RX introduces nonnegligible errors in the OP performance that can exceed 20% under several communication scenarios. It is further demonstrated that the effects by cascaded multipath fading conditions are particularly detrimental as they typically result in considerable performance losses of around or over an order of magnitude.**

***Index Terms*—Cascaded fading channels, hardware-constrained communications, I/Q imbalance, multicarrier communications, N^* Nakagami-m fading channels, outage probability (OP), single-carrier communications, vehicle-to-vehicle (V2V) communications.**

Manuscript received May 28, 2015; revised November 16, 2015; accepted January 4, 2016. Date of publication January 12, 2016; date of current version November 10, 2016. This work was supported by the Academy of Finland under Project 284694 and Project 288670. Part of this work was presented at IEEE PIMRC'16, Hong Kong. The review of this paper was coordinated by Prof. T. Kuerner.

A.-A. A. Boulogeorgos and G. K. Karagiannidis are with the Department of Electrical and Computer Engineering, Aristotle University of Thessaloniki, Thessaloniki 541 24, Greece (e-mail: ampoulog@auth.gr; geokarag@auth.gr).

P. C. Sofotasios is with the Department of Electronics and Communications Engineering, Tampere University of Technology, Tampere 33101, Finland, with the Department of Electrical and Computer Engineering, Khalifa University, Abu Dhabi, UAE, and also with the Department of Electrical and Computer Engineering, Aristotle University of Thessaloniki, Thessaloniki 541 24, Greece (e-mail: p.sofotasios@ieee.org).

B. Selim is with the Department of Electrical and Computer Engineering, Khalifa University, Abu Dhabi, UAE (e-mail: bassant.selim@kustar.ac.ae).

S. Muhaidat is with the Department of Electrical and Computer Engineering, Khalifa University, Abu Dhabi, UAE, and also with the Centre for Communication Systems Research, Department of Electronic Engineering, University of Surrey, Guildford GU2 7XH, U.K. (e-mail: muhaidat@ieee.org).

M. Valkama is with the Department of Electronics and Communications Engineering, Tampere University of Technology, Tampere 33101, Finland (e-mail: mikko.e.valkama@tut.fi).

Digital Object Identifier 10.1109/TVT.2016.2516901

I. Introduction

THE ever-increasing demand for high-data-rate applications and multimedia services has led to the development of flexible and software-configurable transceivers that are capable of supporting the desired quality of service requirements. In this context, the direct-conversion architecture of such systems provides an attractive front-end solution as it requires neither external intermediate frequency filters nor image rejection filters [1], [2]. Instead, the essential image rejection is achieved through signal processing methods [3]. Direct-conversion architectures are low cost and can be easily integrated on chip, which render them excellent candidates for modern wireless technologies [4]–[6]. However, direct-conversion transceivers are typically sensitive to front-end related impairments, which are often inevitable due to components mismatch and manufacturing defects [7], [8]. An indicative example is the in-phase and quadrature (I/Q) imbalance (IQI), which corresponds to the amplitude and phase mismatch between the I and Q branches of a transceiver that ultimately leads to imperfect image rejection that incurs considerable performance degradation [3], [9], [10].

It is also widely known that, due to the different nature of fading conditions, several statistical models have been proposed for characterizing and modeling fading envelopes under short-term, long-term, and composite fading channels. For example, the Nakagami-m and lognormal distributions have been proposed to account for short-term fading, also known as multipath fading, and long-term fading, also known as shadowing, respectively. Likewise, several composite fading models have been proposed for accounting for the simultaneous occurrence of multipath fading and shadowing effects (see [11]–[21] and references therein). In the same context, multiplicative cascaded fading models have been more recently introduced in [22]–[24]. The physical interpretation of these models is justified by considering received signals generated by the product of a large number of rays reflected via N statistically independent scatterers [22]. Based on this, the N^* Nakagami-m distribution was introduced in [23] corresponding to the product of N statistically independent but not necessarily identically distributed Nakagami-m random variables. This model is generic as it includes several special cases of more elementary cascaded fading models. For example, for the specific case of $N = 2$ and $m = 1$, it reduces to the double Rayleigh distribution, which has been shown useful in modeling fading effects in mobile-to-mobile communications [25].

0018-9545 © 2016 IEEE. Personal use is permitted, but republication/redistribution requires IEEE permission.
See http://www.ieee.org/publications_standards/publications/rights/index.html for more information.

A. Related Work

In spite of the paramount importance of radio frequency (RF) front-end on the performance of wireless communication systems, the detrimental effects of RF impairments have been overlooked in the vast majority of reported analyses. The effect of RF impairments, which is modeled as independent and identically distributed (i.i.d.) additive Gaussian noise, was investigated in [26]–[32]. In [33], the impact of IQI on the performance of orthogonal frequency division multiplexing (OFDM) systems was investigated. In particular, a signal-to-interference-plus-noise ratio (SINR) expression was evaluated, considering transmitter (TX)-only IQI, receiver (RX)-only IQI, and joint TX/RX IQI, with equal levels of IQI at the TX and RX ends. Likewise, the effects of IQI on multi-carrier receivers was analyzed in [34], [35]; specifically, the authors in [34] analyzed the impact of the IQI on the bit error rate (BER) performance of an OFDM based system with M-ary quadrature amplitude modulation (M-QAM), whereas the case of received OFDM signals subject to an I/Q imbalanced transceiver was derived in [35], along with a respective compensation algorithm.

In the context of cooperative communications, the performance of amplify-and-forward dual-hop relay systems under IQI was thoroughly investigated in [36]–[42]. In more detail, novel analytical expressions for the symbol error probability (SEP) over Rayleigh fading channels were derived in [36]–[38]. In the former, IQI was assumed only at the destination node, whereas upper and lower bounds for the respective SEP were reported in [37] and [38] for the case of joint TX/RX IQI. Likewise, the authors in [39] derived analytic expression for the outage probability (OP), considering independent and non-identical Nakagami-*m* fading channels, joint TX/RX IQI at the relay nodes and ideal RF front-ends at the source and destination. Moreover, the case of dual-hop opportunistic OFDM in the presence of IQI in all nodes was addressed in [40], where the OP was derived considering statistically independent, frequency-selective channels in all wireless links.

The effects of IQI in the context of two way amplify-and-forward relaying and multiple-input multiple-output (MIMO) systems were investigated in [41]–[46], respectively. Specifically, in [41], [42] and [43]–[46], the effects of IQI in two-way amplify-and-forward relaying systems for the case of independent nonidentically distributed Nakagami-m fading channels were studied. Furthermore, the authors in [43] investigated the impact of IQI in single-carrier MIMO systems and proposed a baseband compensation method, whereas the authors in [44] analyzed the performance degradation of both TX and RX IQI in a space division multiplexing based MIMO OFDM system, where the symbol error rate (SER) performance results were derived for the case of Rayleigh multipath fading channels. Finally, in [45], the effects of IQI in maximum ratio transmission beamforming OFDM systems were investigated, whereas, in [46], a low-complexity IQI compensation method for MIMO OFDM systems was proposed.

B. Contribution

To the best of the authors' knowledge, the detrimental effects of IQI in digital communications over cascaded fading channels have not been addressed in the open technical literature. Motivated by this, this paper is devoted to the quantification and analysis of IQI on the performance of wireless transmission over cascaded Nakagami-m fading channels. The technical contribution of this paper is outlined as follows:

- Novel analytic expressions are derived for the OP in single-carrier systems over N^* Nakagami-m fading channels for the following three scenarios: 1) IQI at the TX only; 2) IQI at the RX only; and 3) joint IQI at the TX/RX.
- The above OP analysis is extended to a multicarrier scenario by additionally taking into account the impact of the presence or the absence of a signal at the mirror frequency channel.
- The offered analytic results along with useful deduced special cases are readily applied in the context of vehicle-to-vehicle (V2V) communication scenarios, which provides explicit justification of their overall importance and practical usefulness.
- A simple and tight lower bound is additionally proposed for the case of RX IQI in the multicarrier scenario. To this effect, a lower bound for the OP is observed in the corresponding cases of RX IQI and joint TX/RX IQI.

C. Organization and Notations

The remainder of this paper is organized as follows. Section II presents the single-carrier and multicarrier system models for all possible configurations of ideal/impaired TX/RX. Section III is devoted to the derivation of the novel analytic expressions for the corresponding OP metrics. Section IV demonstrates an application of the offered results in V2V communications over N^* Nakagami-m channels. Respective numerical results and discussions are provided in Section V, whereas closing remarks are provided in Section VI.

Notations: Unless otherwise stated, $(\cdot)^*$ denotes conjugation, whereas $\Re\{x\}$ and $\Im\{x\}$ represent the real and imaginary parts of x, respectively. Furthermore, the $\mathbb{E}[\cdot]$ and $|\cdot|$ operators denote statistical expectation and absolute value operations, respectively.

II. System and Signal Model

This Section revisits the ideal signal model, which is, henceforth, referred to as ideal RF, as well as the realistic IQI signal models in both single-carrier and multicarrier direct-conversion TX and RX scenarios for the case that TX and RX are equipped with a single antenna.

A. Ideal RF Front End

We assume a signal s transmitted over a flat wireless channel h with additive white Gaussian noise (AWGN) n. The received RF signal is passed through various processing stages, also known as the RF front-end of the RX. These stages include filtering, amplification, analog I/Q demodulation, downconversion to baseband, and sampling. To this effect, the corresponding baseband equivalent received signal can be expressed as

$$r_{\text{ideal}} = hs + n \tag{1}$$

where h is the channel coefficient and n denotes the circularly symmetric complex AWGN. It is assumed that the transmitted signal experiences cascaded fading conditions characterized by a N^* Nakagami-m process, which is composed of $N \geq 1$ independent, but not necessarily identical, Nakagami-m random variables. Based on this, the instantaneous signal-to-noise ratio (SNR) per symbol at the RX input can be given by

$$\gamma_{\text{ideal}} = \frac{E_s}{N_0}|h|^2 \tag{2}$$

where E_s denotes the energy per transmitted symbol, and N_0 is the single-sided AWGN power spectral density. Therefore, the corresponding average SNR is

$$\overline{\gamma} = \frac{E_s}{N_0}\prod_{i=1}^{N}\Omega_i \tag{3}$$

with Ω_i denoting the scaling parameter of the ith Nakagami-m process [23].

In the case of multicarrier systems, the corresponding baseband equivalent received signal at the kth carrier is represented as follows:

$$r_{\text{id}}(k) = h(k)s(k) + n(k) \tag{4}$$

where $s(k)$ is the transmitted signal at the kth carrier, whereas $h(k)$ and $n(k)$ denote the corresponding channel coefficient and the circular symmetric complex AWGN, respectively. Hence, the corresponding instantaneous and average SNRs can be represented as follows:

$$\gamma_{\text{id}}(k) = \frac{E_s}{N_0}|h(k)|^2 \tag{5}$$

and

$$\overline{\gamma}_{\text{id}}(k) = \frac{E_s}{N_0}\prod_{i=1}^{N}\Omega_i(k) \tag{6}$$

respectively.

B. I/Q Imbalance Model

The time-domain baseband representation of the IQI impaired signal is given by [5]

$$g_{\text{IQI}} = K_1^{t/r}g_{\text{id}} + K_2^{t/r}g_{\text{id}}^* \tag{7}$$

where g_{id} denotes the baseband IQI-free signal, and g_{id}^* arises due to the involved IQI effects. Furthermore, the IQI coefficients $K_1^{t/r}$ and $K_2^{t/r}$ are expressed as

$$K_1^{t/r} = \frac{1}{2}\left(1 + \epsilon^{t/r}e^{\pm j\phi^{t/r}}\right) \tag{8}$$

and

$$K_2^{t/r} = \frac{1}{2}\left(1 - \epsilon^{t/r}e^{\mp j\phi^{t/r}}\right) \tag{9}$$

where the positive and negative signs in (8) and the t/r superscripts denote the upconversion and downconversion processes, respectively, whereas the $\epsilon^{t/r}$ and $\phi^{t/r}$ terms account for the TX/RX amplitude and phase mismatch, respectively. It is also noted that the IQI parameters are algebraically linked to each other as follows:

$$K_2^{t/r} = 1 - \left(K_1^{t/r}\right)^*. \tag{10}$$

The $K_1^{t/r}$ and $K_2^{t/r}$ coefficients are associated with the corresponding image rejection ratio (IRR), which determines the amount of attenuation of the image frequency band and is expressed as

$$\text{IRR}_{t/r} = \frac{\left|K_1^{t/r}\right|^2}{\left|K_2^{t/r}\right|^2}. \tag{11}$$

It is recalled here that for practical analog RF front-end electronics, the value of the IRR is typically in the range of 20–40 dB [2], [4], [31], [47]–[50]. Furthermore, the second term $K_2^{t/r}g_{\text{id}}^*$ is caused by the associated imbalances, and in the case of single-carrier transmission, it represents the self-interference effect, whereas in multicarrier transmission, it denotes the image *aliasing* effect, which results to crosstalk between the mirror frequencies in the downconverted signal. This is because, in general, complex conjugate in the time domain corresponds to complex conjugate and mirroring in the frequency domain. Therefore, the spectrum of the imbalance signal at the kth carrier becomes $G_{IQI}^{t/r}(k) = K_1^{t/r}G(k) + K_2^{t/r}G^*(-k)$, where $G(k)$ and $G(-k)$ denote the spectrum of the IQI-free signal at the k and $-k$ carriers, respectively.

C. Single-Carrier Systems Impaired by IQI

Here, we present the signal model for single-carrier transmission in which the TX and/or the RX suffers from IQI.

1) TX Impaired by IQI: In this scenario, it is assumed that TX experiences IQI, whereas the RF front-end of the RX is ideal. To this effect, it follows from (7) that the baseband equivalent transmitted signal is expressed as

$$s_{\text{IQI}} = K_1^t s + K_2^t s^* \tag{12}$$

whereas the baseband equivalent received signal is given by

$$r_{\text{IQI}}^t = hs_{\text{IQI}} + n \tag{13}$$

$$= K_1^t hs + K_2^t hs^* + n. \tag{14}$$

Furthermore, the instantaneous SINR per symbol at the input of the RX is expressed as

$$\gamma = \frac{|K_1^t|^2|h|^2E_s}{|K_2^t|^2|h|^2E_s + N_0} \tag{15}$$

which, after basic algebraic manipulations, can be rewritten as follows:

$$\gamma = \frac{1}{\frac{1}{\text{IRR}_t} + \frac{1}{|K_1^t|^2}\frac{1}{\gamma_{\text{ideal}}}}. \tag{16}$$

In the context of direct-conversion transmitter, the IQI effect can be considered as the so-called self-image problem, which is the case when the baseband equivalent transmitted signal is essentially interfered by its own complex conjugate [7].

2) RX Impaired by IQI: In this scenario, it is assumed that the RX experiences IQI, whereas the TX RF front-end is ideal. Based on (7), the baseband equivalent received signal is given by

$$r = K_1^r h s + K_2^r h^* s^* + K_1^r n + K_2^r n^*. \tag{17}$$

The corresponding instantaneous SINR per symbol at the input of the RX is expressed as

$$\gamma = \frac{|K_1^r|^2 |h|^2 E_s}{|K_2^r|^2 |h|^2 E_s + \left(|K_1^r|^2 + |K_2^r|^2\right) N_0} \tag{18}$$

which after basic algebraic manipulations can equivalently be expressed as

$$\gamma = \frac{1}{\frac{1}{\mathrm{IRR}_r} + \left(1 + \frac{1}{\mathrm{IRR}_r}\right) \frac{1}{\gamma_{\mathrm{ideal}}}}. \tag{19}$$

3) Joint TX/RX Impaired by IQI: In this scenario, it is assumed that both TX and RX experience IQI. To this effect and based on (7), it follows that the baseband equivalent received signal can be expressed as:

$$r = (\xi_{11} h + \xi_{22} h^*) s + (\xi_{12} h + \xi_{21} h^*) s^* + K_1^r n + K_2^r n^* \tag{20}$$

where

$$\xi_{11} = K_1^r K_1^t \tag{21}$$
$$\xi_{22} = K_2^r \left(K_2^t\right)^* \tag{22}$$
$$\xi_{12} = K_1^r K_2^t \tag{23}$$

and

$$\xi_{21} = K_2^r \left(K_1^t\right)^*. \tag{24}$$

Based on this, the instantaneous SINR per symbol at the input of the RX is given by

$$\gamma = \frac{|Z|^2 E_s}{|W|^2 E_s + \left(|K_1^r|^2 + |K_2^r|^2\right) N_0} \tag{25}$$

with

$$|Z|^2 = |\xi_{11} h + \xi_{22} h^*|^2 \tag{26}$$
$$|W|^2 = |\xi_{12} h + \xi_{21} h^*|^2 \tag{27}$$
$$= |\xi_{12}|^2 |h|^2 + |\xi_{21}|^2 |h|^2 + 2\Re\{\xi_{12}\xi_{21} h^2\} \tag{28}$$

whereas

$$\frac{|\xi_{22}|^2}{|\xi_{11}|^2} = \frac{1}{\mathrm{IRR}_r \mathrm{IRR}_t} \tag{29}$$

which practically lies in the range of $[-43, -28$ dB$]$. As a result, it can be accurately assumed that

$$|Z|^2 \approx |\xi_{11}|^2 |h|^2 \tag{30}$$

whereas due to the inequality

$$2\Re\{\xi_{12}\xi_{21} h^2\} \ll |\xi_{12}|^2 |h|^2 + |\xi_{21}|^2 |h|^2 \tag{31}$$

equation (28) can be accurately represented as

$$|W|^2 \approx |\xi_{12}|^2 |h|^2 + |\xi_{21}|^2 |h|^2. \tag{32}$$

To this effect, it follows that (25) can also be rewritten as

$$\gamma \approx \frac{|\xi_{11}|^2}{|\xi_{12}|^2 + |\xi_{21}|^2 + \left(|K_1^r|^2 + |K_2^r|^2\right) \frac{1}{\gamma_{\mathrm{ideal}}}}. \tag{33}$$

It is noted here that (33) is particularly accurate since the involved relative error does not exceed 1%.

D. Multicarrier Systems Impaired by IQI

In the case of multicarrier transmission, we assume that multiple RF carriers are downconverted to the baseband by means of wideband direct conversion, where the RF spectrum is translated to the baseband in a single downconversion [4]. For notational convenience, we denote the set of channels as $\mathbf{S}_K = \{-K, \ldots, -1, 1, \ldots, K\}$ and the baseband equivalent IQI-free transmitted signal at the kth carrier as $s(k)$. In addition, the $\theta \in \{0, 1\}$ parameter indicates the existence of a signal at channel $-k$.

1) TX Impaired by IQI: In this scenario, it is assumed that the RF front-end of the RX is ideal, whereas the TX experiences IQI. Therefore, with the aid of (7), it follows that the baseband equivalent transmitted signal in the kth carrier is expressed as

$$s_{\mathrm{IQI}}(k) = K_1^t s(k) + \theta K_2^t s^*(-k). \tag{34}$$

Notably, (34) exhibits that IQI causes the transmitted baseband equivalent signal at the carrier k, i.e., $s(k)$, to be distorted by its image signal at carrier $-k$, $s^*(-k)$. In other words, in a multicarrier system, the effects of IQI result in crosstalk between the mirror frequencies in the downconverted signal [47]. To this effect, the corresponding baseband received signal becomes

$$r(k) = h(k) s_{\mathrm{IQI}}(k) + n(k) \tag{35}$$

which, with the aid of (34), can be equivalently rewritten as follows:

$$r(k) = K_1^t h(k) s(k) + K_2^t h(k) s^*(-k) + n(k). \tag{36}$$

Moreover, the corresponding instantaneous SINR per symbol at the input of the RX is given by

$$\gamma(k) = \frac{|K_1^t|^2 |h(k)|^2 E_s}{\theta |K_2^t|^2 |h(k)|^2 E_s + N_0} \tag{37}$$

which, after carrying out basic algebraic manipulations, can be expressed as

$$\gamma(k) = \frac{1}{\theta \frac{1}{\mathrm{IRR}_t} + \frac{1}{|K_1^t|^2} \frac{1}{\gamma_{\mathrm{id}}(k)}}. \tag{38}$$

2) RX Impaired by IQI: In this scenario, it is assumed that the RF front-end of the TX is ideal, whereas the RX experiences IQI. Hence, by recalling once more (7), the baseband equivalent received signal in the kth carrier can be represented as follows:

$$r(k) = K_1^r h(k) s(k) + \theta K_2^r h^*(-k) s^*(-k) + K_1^r n(k) + K_2^r n^*(-k). \tag{39}$$

With the aid of the given expression, it is shown that IQI is the reason that the received baseband equivalent signal at the kth

carrier, $s(k)$, is interfered by the image signal at the carrier $-k$, $s^*(-k)$. The instantaneous SINR per symbol at the input of the RX is expressed as

$$\gamma(k) = \frac{|K_1^r|^2 |h(k)|^2 E_s}{|K_2^r|^2 |h(-k)|^2 E_s + \left(|K_1^r|^2 + |K_2^r|^2\right) N_0} \quad (40)$$

$$= \frac{\gamma_{\rm id}(k)}{\theta \frac{\gamma_{\rm id}(-k)}{{\rm IRR}_r} + \left(1 + \frac{1}{{\rm IRR}_r}\right)} \quad (41)$$

where $\gamma_{\rm id}(k)$ is given by (5), and

$$\gamma_{\rm id}(-k) = \frac{|h(-k)|^2 E_s}{N_0}. \quad (42)$$

3) Joint TX/RX Impaired by IQI: Finally, it is assumed that both the TX and RX experience IQI. Thus, with the aid of (7) and after some basic algebraic manipulations, the baseband equivalent received signal can be expressed as follows:

$$\begin{aligned} r(k) = &\left(\xi_{11} h(k) + \xi_{22} h^*(-k)\right) s(k) \\ &+ \left(\xi_{12} h(k) + \xi_{21} h^*(-k)\right) s^*(-k) \\ &+ K_1^r n(k) + K_2^r n^*(-k) \end{aligned} \quad (43)$$

which indicates that IQI renders the received baseband equivalent signal at the kth carrier, $s(k)$, subject to interference by its image signal at the carrier $-k$, $s^*(-k)$. Therefore, the corresponding instantaneous SINR per symbol at the input of the RX is given by

$$\gamma(k) = \frac{|Z_{\rm MC}(k)|^2 E_s}{|W_{\rm MC}(k)|^2 E_s + \left(|K_1^r|^2 + |K_2^r|^2\right) N_0} \quad (44)$$

where

$$|Z_{\rm MC}(k)|^2 = |\xi_{11} h(k) + \xi_{22} h^*(-k)|^2 \quad (45)$$

and

$$|W_{\rm MC}(k)|^2 = |\xi_{12} h(k) + \xi_{21} h^*(-k)|^2 . \quad (46)$$

Likewise, (45) can be accurately expressed as

$$|Z_{\rm MC}(k)|^2 \approx |\xi_{11}|^2 |h(k)|^2 . \quad (47)$$

In addition, it is noted that the correlation between the channel responses at the kth carrier and its image is small due to their large spectral separation. To this effect, it is realistic to assume them statistically independent, which satisfies the following expression:

$$\mathbb{E}\left[\Re\left\{\xi_{12}\xi_{21}^* h(k) h^*(-k)\right\}\right] \approx 0. \quad (48)$$

Based on this, $|W_{\rm MC}(k)|^2$ can be tightly approximated as

$$|W_{\rm MC}(k)|^2 \approx |\xi_{12}|^2 |h(k)|^2 + |\xi_{21}|^2 |h^*(-k)|^2 . \quad (49)$$

Based on the above analysis, it immediately follows that (44) can be expressed as

$$\gamma(k) \approx \frac{|\xi_{11}|^2 \gamma_{\rm id}(k)}{\theta |\xi_{12}|^2 \gamma_{\rm id}(k) + \theta |\xi_{21}|^2 \gamma_{\rm id}(-k) + |K_1^r|^2 + |K_2^r|^2} \quad (50)$$

which is a particularly accurate and simple representation. In general, we wish to emphasize that the nature of IQI is clearly different in the single-carrier and multicarrier transmission cases. This is primarily because, in the multicarrier case, the image carrier carries an independent data symbol, whereas in the single-carrier case, the image is the complex conjugate of the signal itself. Furthermore, the fading at mirror carriers is generally different, whereas in the single-carrier case, the signal and its own conjugate experience the same fading process.

III. Outage Probability Over Cascaded Fading Channels

It is recalled that the OP can be defined as the probability that the symbol error rate is greater than a certain quality of service requirement and is computed as the probability that the instantaneous SNR or SINR falls below the corresponding predetermined threshold [51]. In what follows, we derive a novel analytical framework for the OP over N^* Nakagami-m fading channels subject to the aforementioned IQI scenarios in both single-carrier and multicarrier systems. The offered analytic expressions are validated through extensive comparisons with respective results from computer simulations.

A. Ideal RF Front End

In the case of N^* Nakagami-m fading channels, the cumulative distribution function (CDF) of $\gamma_{\rm ideal}$ is given by [23, Eq. (13)]

$$\begin{aligned} F_{\gamma_{\rm ideal}}(\gamma) = &\frac{1}{\prod_{i=1}^N \Gamma(m_i)} \\ &\times G_{1,N+1}^{N,1}\left(\frac{\gamma}{\overline{\gamma}} \prod_{i=1}^N m_i \,\middle|\, \begin{matrix} 1 \\ m_1, m_2, \ldots, m_N, 0 \end{matrix}\right) \end{aligned} \quad (51)$$

where $\Gamma(\cdot)$ and $G_{s,t}^{v,w}(\cdot)$ denote the gamma function and the Meijer G-function [52], respectively. Based on this, the corresponding probability density function (PDF) of $\gamma_{\rm ideal}$ is expressed as [23, Eq. (14)], namely

$$f_{\gamma_{\rm ideal}}(\gamma) = \frac{G_{0,N}^{N,0}\left(\frac{\gamma}{\overline{\gamma}} \prod_{i=1}^N m_i \,\middle|\, \begin{matrix} - \\ m_1, m_2, \ldots, m_N \end{matrix}\right)}{\gamma \prod_{i=1}^N \Gamma(m_i)}. \quad (52)$$

B. Single-Carrier Systems Impaired by IQI

1) TX Impaired by IQI: Using (16) and (51), it follows that the OP can be expressed as

$$P_{\rm out} = F_{\gamma_{\rm ideal}}\left(\frac{1}{|K_1^t|^2 \left(\frac{1}{\gamma_{\rm th}} - \frac{1}{{\rm IRR}_t}\right)}\right) \quad (53)$$

with $\gamma_{\rm th} \leq {\rm IRR}_t$.

2) RX Impaired by IQI: With the aid of (19) and (51), the corresponding OP is given by

$$P_{\text{out}} = F_{\gamma_{\text{ideal}}}\left(\frac{1+\frac{1}{\text{IRR}_r}}{\frac{1}{\gamma_{\text{th}}}-\frac{1}{\text{IRR}_r}}\right) \tag{54}$$

with $\gamma_{\text{th}} \leq \text{IRR}_r$.

3) Joint TX/RX Impaired by IQI: Using (33) and (51), the OP in this case is expressed as

$$P_{\text{out}} = F_{\gamma_{\text{ideal}}}\left(\frac{|K_1^r|^2+|K_2^r|^2}{\frac{|\xi_{11}|^2}{\gamma_{\text{th}}}-(|\xi_{12}|^2+|\xi_{21}|^2)}\right) \tag{55}$$

with $\gamma_{\text{th}} \leq \frac{|\xi_{11}|^2}{|\xi_{12}|^2+|\xi_{21}|^2}$.

C. Multicarrier Systems Impaired by IQI

Similar analytic expressions can be derived for the case of multicarrier transmission.

1) TX Impaired by IQI: Based on the signal model in Section II-D1 and assuming a known θ, it immediately follows that

$$F_\gamma(\gamma_{\text{th}}|\theta) = F_{\gamma_{\text{ideal}}}\left(\frac{1}{|K_1^t|^2\left(\frac{1}{\gamma_{\text{th}}}-\theta\frac{1}{\text{IRR}_t}\right)}\right) \tag{56}$$

with $\gamma_{\text{th}} \leq \text{IRR}_t$.

It is also assumed here that θ follows a Bernoulli distribution with CDF, i.e.,

$$P_r(\theta) = \begin{cases} q, & \theta = 1 \\ 1-q, & \theta = 0 \end{cases} \tag{57}$$

and $q \in [0,1]$. To this effect, the corresponding unconditional OP can be expressed as follows:

$$P_{\text{out}} = qF_{\gamma_{\text{ideal}}}\left(\frac{1}{|K_1^t|^2\left(\frac{1}{\gamma_{\text{th}}}-\frac{1}{\text{IRR}_t}\right)}\right) + (1-q)F_{\gamma_{\text{ideal}}}\left(\frac{\gamma_{\text{th}}}{|K_1^t|^2}\right). \tag{58}$$

2) RX Impaired by IQI: Based on the signal model presented in Section II-D2, assuming a given image channel realization, SNR $\gamma_{\text{ideal}}(-k)$, and a known θ, it follows that

$$F_\gamma\left(\gamma_{\text{th}}|\gamma_{\text{ideal}}(-k),\theta\right) = F_{\gamma_{\text{ideal}}}\left(\left(\theta\frac{\gamma_{\text{ideal}}(-k)}{\text{IRR}_r}+1+\frac{1}{\text{IRR}_r}\right)\gamma_{\text{th}}\right). \tag{59}$$

If $\theta = 1$, the unconditional cdf can be expressed as follows:

$$F_\gamma(\gamma_{\text{th}}|\theta=1) = \int_0^\infty F_{\gamma_{\text{ideal}}}\left(\left(\frac{x}{\text{IRR}_r}+1+\frac{1}{\text{IRR}_r}\right)\gamma_{\text{th}}\right)f_{\gamma_{\text{ideal}}}(x)\,\mathrm{d}x. \tag{60}$$

By also taking into consideration (51) and (52), the given expression can be rewritten as (61), shown at the bottom of the page, which after some basic algebraic manipulations can be equivalently expressed as follows:

$$F_\gamma(\gamma_{\text{th}}|\theta=1) = \frac{1}{\left(\prod_{i=1}^N\Gamma(m_i)\right)^2} \times \int_0^\infty \frac{1}{y}G_{1,N+1}^{N,1}\left(y+c\,\middle|\,\begin{matrix}1\\ m_1,m_2,\ldots,m_N,0\end{matrix}\right) \times G_{0,N}^{N,0}\left(\frac{d}{b}y\,\middle|\,\begin{matrix}-\\ m_1,m_2,\ldots,m_N,0\end{matrix}\right)\mathrm{d}y \tag{62}$$

where

$$y = bx \tag{63}$$

$$b = \frac{\gamma_{\text{th}}}{\overline{\gamma}}\frac{1}{\text{IRR}_r}\prod_{i=1}^N m_i \tag{64}$$

$$c = \frac{\gamma_{\text{th}}}{\overline{\gamma}}\left(1+\frac{1}{\text{IRR}_r}\right)\prod_{i=1}^N m_i \tag{65}$$

and

$$d = \frac{1}{\overline{\gamma}}\prod_{i=1}^N m_i. \tag{66}$$

Importantly, (62) can be expressed in terms of the Meijer G-function in [52] yielding (67), shown at the bottom of the next page. Likewise, when $\theta = 0$, the corresponding unconditional CDF can be readily deduced, namely

$$F_\gamma(\gamma_{\text{th}}|\theta=0) = F_{\gamma_{\text{ideal}}}\left(\left(1+\frac{1}{\text{IRR}_r}\right)\gamma_{\text{th}}\right). \tag{68}$$

Based on the above analysis, the corresponding unconditional OP is expressed as (69), shown at the bottom of the next page.

$$F_\gamma(\gamma_{\text{th}}|\theta=1) = \frac{1}{\left(\prod_{i=1}^N\Gamma(m_i)\right)^2}\int_0^\infty x^{-1}G_{0,N}^{N,0}\left(\frac{x}{\overline{\gamma}}\prod_{i=1}^N m_i\,\middle|\,\begin{matrix}-\\ m_1,m_2,\ldots,m_N\end{matrix}\right) \times G_{1,N+1}^{N,1}\left(\left(\frac{x}{\text{IRR}_r}+1+\frac{1}{\text{IRR}_r}\right)\frac{\gamma_{\text{th}}}{\overline{\gamma}}\prod_{i=1}^N m_i\,\middle|\,\begin{matrix}1\\ m_1,m_2,\ldots,m_N,0\end{matrix}\right)\mathrm{d}x \tag{61}$$

3) Joint TX/RX Impaired by IQI: By recalling (50) and assuming a given $\gamma_{\rm ideal}(-k)$ and a known θ, it immediately follows that

$$F_\gamma\left(\gamma_{\rm th}|\gamma_{\rm ideal}(-k),\theta\right) = F_{\gamma_{\rm ideal}}\left(\frac{\gamma_{\rm th}\left(\theta|\xi_{21}|^2\gamma_{\rm ideal}(-k)+|K_1^r|^2+|K_2^r|^2\right)}{|\xi_{11}|^2-\theta\gamma_{\rm th}|\xi_{12}|^2}\right). \tag{70}$$

Likewise, in the case of $\theta=1$, the unconditional CDF can be formulated as

$$F_\gamma(\gamma_{\rm th}|\theta=1) = \int_0^\infty F_{\gamma_{\rm ideal}}\left(\frac{\gamma_{\rm th}\left(|\xi_{21}|^2x+|K_1^r|^2+|K_2^r|^2\right)}{|\xi_{11}|^2-\gamma_{\rm th}|\xi_{12}|^2}\right) f_{\gamma_{\rm ideal}}(x){\rm d}x \tag{71}$$

which, with the aid of (51) and (52) and by carrying out some basic algebraic manipulations, can be equivalently expressed as (72), shown at the bottom of the page. Note that, in (72), y, g, l, and u stand for

$$y = gx \tag{73}$$

$$g = \frac{|\xi_{21}|^2\gamma_{\rm th}}{\overline{\gamma}\left(|\xi_{11}|^2-\gamma_{\rm th}|\xi_{12}|^2\right)}\prod_{i=1}^N\Gamma(m_i) \tag{74}$$

$$l = \frac{\left(|K_1^r|^2+|K_2^r|^2\right)\gamma_{\rm th}}{\overline{\gamma}\left(|\xi_{11}|^2-\gamma_{\rm th}|\xi_{12}|^2\right)}\prod_{i=1}^N\Gamma(m_i) \tag{75}$$

and

$$u = \frac{1}{\overline{\gamma}}\prod_{i=1}^N m_i. \tag{76}$$

It is evident that (62) can be also expressed in terms of the Meijer G-function [52], namely (77), shown at the bottom of the page. In the same context, when $\theta=0$, the corresponding unconditional CDF is given by

$$F_\gamma(\gamma_{\rm th}|\theta=0) = F_{\gamma_{\rm ideal}}\left(\frac{|K_1^r|^2+|K_2^r|^2}{|\xi_{11}|^2}\gamma_{\rm th}\right). \tag{78}$$

To this effect, it immediately follows that the unconditional OP can be expressed as (79), shown at the bottom of the next page.

$$F_\gamma(\gamma_{\rm th}|\theta=1) \simeq \sum_{k=0}^p \frac{(-1)^k\gamma_{\rm th}^k}{\overline{\gamma}^k k!}\left(1+\frac{1}{{\rm IRR}_r}\right)^k\left(\prod_{i=1}^N m_i\right)^k \times G_{N+2,N+2}^{N+1,N+1}\left(\frac{{\rm IRR}_r}{\gamma_{\rm th}}\,\middle|\,\begin{matrix}1,k-m_1+1,k-m_2+1,\ldots,k-m_N+1,k+1\\ m_1,m_2,\ldots,m_N,k,k+1,0\end{matrix}\right) \tag{67}$$

$$P_{\rm out} = q\sum_{k=0}^p \frac{(-1)^k\gamma_{\rm th}^k}{\overline{\gamma}^k k!}\left(1+\frac{1}{{\rm IRR}_r}\right)^k\left(\prod_{i=1}^N m_i\right)^k G_{N+2,N+2}^{N+1,N+1}\left(\frac{{\rm IRR}_r}{\gamma_{\rm th}}\,\middle|\,\begin{matrix}1,k-m_1+1,k-m_2+1,\ldots,k-m_N+1,k+1\\ m_1,m_2,\ldots,m_N,k,k+1,0\end{matrix}\right) + (1-q)\frac{1}{\prod_{i=1}^N\Gamma(m_i)}G_{1,N+1}^{N,1}\left(\frac{\left(1+\frac{1}{{\rm IRR}_r}\right)\gamma_{\rm th}}{\overline{\gamma}}\prod_{i=1}^N m_i\,\middle|\,\begin{matrix}1\\ m_1,m_2,\ldots,m_N,0\end{matrix}\right) \tag{69}$$

$$F_\gamma(\gamma_{\rm th}|\theta=1) = \frac{1}{\left(\prod_{i=1}^N\Gamma(m_i)\right)^2}\int_0^\infty \frac{1}{z}G_{1,N+1}^{N,1}\left(z+l\,\middle|\,\begin{matrix}1\\ m_1,m_2,\ldots,m_N,0\end{matrix}\right)G_{0,N}^{N,0}\left(\frac{u}{g}z\,\middle|\,\begin{matrix}-\\ m_1,m_2,\ldots,m_N\end{matrix}\right){\rm d}z \tag{72}$$

$$F_\gamma(\gamma_{\rm th}|\theta=1) \simeq \sum_{k=0}^p \frac{(-1)^k\gamma_{\rm th}^k\left(|K_1^r|^2+|K_2^r|^2\right)^k}{k!\overline{\gamma}^k\left(|\xi_{11}|^2-\gamma_{\rm th}|\xi_{12}|^2\right)^k}\left(\prod_{i=1}^N\Gamma(m_i)\right)^k \times G_{N+2,N+2}^{N+1,N+1}\left(\frac{|\xi_{11}|^2-\gamma_{\rm th}|\xi_{12}|^2}{|\xi_{21}|^2\gamma_{\rm th}}\,\middle|\,\begin{matrix}1,k-m_1+1,k-m_2+1,\ldots,k-m_N+1,k+1\\ m_1,m_2,\ldots,m_N,k,k+1,0\end{matrix}\right) \tag{77}$$

Importantly, the offered analytic expressions can be readily computed in popular mathematical software packages such as Maple, Mathematica, and Matlab. Furthermore, it is noted that, to the best of the authors' knowledge, the offered analytic expressions in Section III have not been previously reported in the open technical literature.

IV. Applications in Vehicle-to-Vehicle Communications

It is well known that V2V communications constitute a fundamental part of emerging communication systems. This also includes intelligent transportation systems, which have been attracting considerable attention due to the large number of applications in which they can be effectively deployed. It is recalled that the transmitted signals in V2V communication systems experience fading effects that typically differ from conventional cellular communications scenarios [53], [54]. This difference arises from the moving nature and the position of the involved TX/RX, as well as the presence of reflectors/scatterers in highways and urban environments. As a result, the omnidirectional TX and RX antennas in these systems are located at relatively low elevations; thus, the corresponding wireless channel has been shown to exhibit a nonstationary behavior. As a consequence, the performance of corresponding communication systems is subject to nonnegligible deteriorations in terms of throughput and OP, which becomes particularly problematic in certain communications scenarios including safety applications [55]. To this effect, wireless channels in V2V communications should be accurately characterized and modeled to evaluate the performance of these systems precisely and incorporate the essential techniques that are capable of ensuring the fulfillment of the corresponding application requirements, resulting in efficient and robust wireless transmission. To this end, we consider a V2V communication system, where the TX and RX are equipped with a single antenna. In this context, we evaluate the corresponding OP over cascaded fading channels for both single-carrier and multicarrier direct-conversion transceivers impaired by IQI.

A. Single-Carrier V2V Communication System

The complex fading coefficient of the considered wireless communication link is represented by h and is assumed to be the product of statistically independent, but not necessarily identically distributed, N^* Nakagami-m random variables, namely [53]

$$h = \prod_{i=1}^{N} h_i. \tag{80}$$

It is recalled here that due to the nature of the surrounding environment, the position of the antennas and the mobility of both the TX and RX, the double and triple Nakagami-m distributions have been proven adequate to model fading in basic V2V communications [53]. In what follows, simple analytic expressions are derived for the corresponding measures for these cases that constitute special cases of the more generic N^* Nakagami-m fading distribution and are expressed in a simpler algebraic form.

1) Double Nakagami-m Channel: It is recalled that the envelope PDF of double Nakagami-m channels, i.e., $N = 2$, is given in [23, Eq. (6)]. Based on this and with the aid of [56, Eq. (2.3)], it immediately follows that

$$p_\gamma(\gamma) = \mathcal{A}\gamma^{\frac{m_1+m_2}{2}-1} K_{m_1-m_2}\left(\mathcal{B}\sqrt{\gamma}\right) \tag{81}$$

where $K_n(\cdot)$ denotes the modified Bessel function of the second kind, whereas

$$\mathcal{A} = \frac{2}{\overline{\gamma}^{\frac{m_1+m_2}{2}} \prod_{i=1}^{2} \Gamma(m_i) m_i^{-\frac{m_1+m_2}{2}}} \tag{82}$$

and

$$\mathcal{B} = \frac{2}{\sqrt{\overline{\gamma}}} \prod_{i=1}^{2} \sqrt{m_i}. \tag{83}$$

Based on (81), the corresponding CDF is given by

$$F_\gamma(x) = \mathcal{A} \int_0^\gamma x^{\frac{m_1+m_2}{2}-1} K_{m_1-m_2}\left(\mathcal{B}\sqrt{x}\right) \mathrm{d}x \tag{84}$$

which can be expressed in closed form with the aid of [57, Eq. (1.12.2)] yielding

$$\begin{aligned} F_\gamma(\gamma) =& \frac{\mathcal{A}\gamma^{m_1}\Gamma(m_2-m_1)}{m_1 2^{m_1-m_2}\mathcal{B}^{m_2-m_1}} \\ &\times {}_1F_2\left(m_1; m_1+1, m_1-m_2+1; \frac{\mathcal{B}^2\gamma}{4}\right) \\ &+ \frac{\mathcal{A}\gamma^{m_2}\Gamma(m_1-m_2)}{m_2 2^{1-m_1+m_2}\mathcal{B}^{m_2-m_1}} \\ &\times {}_1F_2\left(m_2; m_2+1, m_2-m_1+1; \frac{\mathcal{B}^2\gamma}{4}\right) \end{aligned} \tag{85}$$

$$\begin{aligned} P_{\mathrm{out}} =& q\sum_{k=0}^{p} \frac{(-1)^k \gamma_{\mathrm{th}}^k \left(|K_1^r|^2 + |K_2^r|^2\right)^k}{k!\overline{\gamma}^k \left(|\xi_{11}|^2 - \gamma_{\mathrm{th}}|\xi_{12}|^2\right)^k} \left(\prod_{i=1}^{N}\Gamma(m_i)\right)^k \\ &\times G_{N+2,N+2}^{N+1,N+1}\left(\frac{|\xi_{11}|^2 - \gamma_{\mathrm{th}}|\xi_{12}|^2}{|\xi_{21}|^2\gamma_{\mathrm{th}}} \middle| \begin{matrix} 1, k-m_1+1, k-m_2+1, \ldots, k-m_N+1, k+1 \\ m_1, m_2, \ldots, m_N, k, k+1, 0 \end{matrix}\right) \\ &+ (1-q)\frac{1}{\prod_{i=1}^{N}\Gamma(m_i)} G_{1,N+1}^{N,1}\left(\frac{|K_1^r|^2 + |K_2^r|^2}{|\xi_{11}|^2\overline{\gamma}}\gamma_{\mathrm{th}}\prod_{i=1}^{N} m_i \middle| \begin{matrix} 1 \\ m_1, m_2, \ldots, m_N, 0 \end{matrix}\right) \end{aligned} \tag{79}$$

where ${}_pF_q(\cdot)$ denotes the generalized hypergeometric function [57]. It is noted here that the given expression is not valid when $m_1 = m_2$ as the gamma function is by definition undefined for zero values of its argument.[1] In the same context as earlier, for the special case that $m_1 - m_2 \pm (1/2) \in \mathbb{N}$, the $K_n(\cdot)$ function in (81) can be expressed according to [52, Eq. (8.468)]. Based on this and by performing the necessary variable transformation, the SNR PDF of the double Nakagami-m fading model can be alternatively expressed as

$$p_\gamma(\gamma) = \sum_{l=0}^{m_1-m_2-\frac{1}{2}} \sqrt{\frac{\pi}{2\mathcal{B}}} \frac{\mathcal{A}\left(m_1-m_2+l-\frac{1}{2}\right)!}{l!\left(m_1-m_2-l-\frac{1}{2}\right)!(2\mathcal{B})^l} \times \gamma^{\frac{m_1+m_2-l}{2}-\frac{5}{4}} \exp(-\mathcal{B}\sqrt{\gamma}) \quad (86)$$

whereas the corresponding CDF is given by

$$F_\gamma(\gamma) = \sum_{l=0}^{m_1-m_2-\frac{1}{2}} \frac{\mathcal{A}\sqrt{\pi}\Gamma\left(m_1-m_2+l+\frac{1}{2}\right)}{l!\Gamma\left(m_1-m_2-l+\frac{1}{2}\right)(2\mathcal{B})^{l+\frac{1}{2}}} \times \int_0^\gamma x^{\frac{m_1+m_2-l}{2}-\frac{5}{4}} \exp(-\mathcal{B}\sqrt{x})\mathrm{d}x. \quad (87)$$

The integral in (87) can be expressed in closed form with the aid of [52, Eq. (8.350.1)]. As a result, by performing the necessary change of variables and substituting in (87), it follows that

$$F_\gamma(\gamma) = \mathcal{A}\sqrt{\pi} \times \sum_{l=0}^{m_1-m_2-\frac{1}{2}} \frac{\Gamma\left(m_1-m_2+l+\frac{1}{2}\right)\gamma\left(m_1-m_2+l+\frac{1}{2},\mathcal{B}\sqrt{\gamma}\right)}{l!2^{l-\frac{1}{2}}\mathcal{B}^{m_1+m_2}\Gamma\left(m_1-m_2-l+\frac{1}{2}\right)} \quad (88)$$

which is also valid for the case that $m_1 - m_2 \pm \frac{1}{2} \in \mathbb{N}$.

To this effect, in the case of single-carrier V2V communication with only TX impaired with IQI, (53) can be straightforwardly expressed as follows:

$$P_{\text{out}} = \frac{1}{\Gamma(m_1)\Gamma(m_2)} \times G_{1,3}^{2,1}\left(\frac{1}{|K_1^t|^2\left(\frac{1}{\gamma_{\text{th}}}-\frac{1}{\text{IRR}_t}\right)\overline{\gamma}}\prod_{i=1}^{2} m_i \,\middle|\, \begin{matrix}1\\ m_1, m_2, 0\end{matrix}\right) \quad (89)$$

[1] In such cases, the corresponding results can be obtained with the aid of the generic analytic expressions in Section III. This is also the case in the respective considered scenarios in Section V.

which, with the aid of (85) and (87), can be equivalently rewritten as (90), shown at the bottom of the page. Likewise, for the special case that $m_1 - m_2 \pm (1/2) \in \mathbb{N}$, it can be further simplified to

$$P_{\text{out}} = \sum_{l=0}^{m_1-m_2-\frac{1}{2}} \frac{2^{\frac{1}{2}-l}\Gamma\left(m_1-m_2+l+\frac{1}{2}\right)}{l!\mathcal{B}^{m_1+m_2}\Gamma\left(m_1-m_2-l+\frac{1}{2}\right)} \times \gamma\left(m_1-m_2+l+\frac{1}{2}, \frac{\mathcal{B}}{|K_1^t|\sqrt{\frac{1}{\gamma_{\text{th}}}-\frac{1}{\text{IRR}_t}}}\right) \quad (91)$$

with $\gamma(a,x)$ denoting the lower incomplete gamma function [57].

In the same context, in the case of only RX impaired with IQI, (54) can be rewritten as

$$P_{\text{out}} = \frac{1}{\Gamma(m_1)\Gamma(m_2)} \times G_{1,3}^{2,1}\left(\frac{1+\frac{1}{\text{IRR}_r}}{\left(\frac{1}{\gamma_{\text{th}}}-\frac{1}{\text{IRR}_r}\right)\overline{\gamma}}\prod_{i=1}^{2} m_i \,\middle|\, \begin{matrix}1\\ m_1, m_2, 0\end{matrix}\right) \quad (92)$$

or alternatively as

$$\begin{aligned} P_{\text{out}} =& \frac{\mathcal{A}\Gamma(m_2-m_1)}{m_1 2^{m_1-m_2}\mathcal{B}^{m_2-m_1}}\left(\frac{1+\frac{1}{\text{IRR}_r}}{\frac{1}{\gamma_{\text{th}}}-\frac{1}{\text{IRR}_r}}\right)^{m_1} \\ &\times {}_1F_2\left(m_1; m_1+1, m_1-m_2+1; \frac{\mathcal{B}^2}{4}\frac{1+\frac{1}{\text{IRR}_r}}{\frac{1}{\gamma_{\text{th}}}-\frac{1}{\text{IRR}_r}}\right) \\ &+ \frac{\mathcal{A}\Gamma(m_1-m_2)}{m_2 2^{1-m_1+m_2}\mathcal{B}^{m_2-m_1}}\left(\frac{1+\frac{1}{\text{IRR}_r}}{\frac{1}{\gamma_{\text{th}}}-\frac{1}{\text{IRR}_r}}\right)^{m_2} \\ &\times {}_1F_2\left(m_2; m_2+1, m_2-m_1+1; \frac{\mathcal{B}^2}{4}\frac{1+\frac{1}{\text{IRR}_r}}{\frac{1}{\gamma_{\text{th}}}-\frac{1}{\text{IRR}_r}}\right) \end{aligned} \quad (93)$$

which is also valid when $m_1 \neq m_2$. Furthermore, for the special case that $m_1 - m_2 \pm (1/2) \in \mathbb{N}$, the OP can be expressed as follows:

$$P_{\text{out}} = \sum_{l=0}^{m_1-m_2-\frac{1}{2}} \frac{\mathcal{A}\sqrt{\pi}\Gamma\left(m_1-m_2+l+\frac{1}{2}\right)}{l!2^{l-\frac{1}{2}}\mathcal{B}^{m_1+m_2}\Gamma\left(m_1-m_2-l+\frac{1}{2}\right)} \times \gamma\left(m_1-m_2+l+\frac{1}{2}, \mathcal{B}\sqrt{\frac{1+\frac{1}{\text{IRR}_r}}{\frac{1}{\gamma_{\text{th}}}-\frac{1}{\text{IRR}_r}}}\right). \quad (94)$$

$$\begin{aligned} P_{\text{out}} =& \left(\frac{1}{|K_1^t|^2\left(\frac{1}{\gamma_{\text{th}}}-\frac{1}{\text{IRR}_t}\right)}\right)^{m_1} \frac{\mathcal{A}\Gamma(m_2-m_1)}{m_1 2^{m_1-m_2}\mathcal{B}^{m_2-m_1}}\,{}_1F_2\left(m_1; m_1+1, m_1-m_2+1; \frac{1}{|K_1^t|^2\left(\frac{\mathcal{B}^2}{4}\frac{1}{\gamma_{\text{th}}}-\frac{1}{\text{IRR}_t}\right)}\right) \\ &+ \left(\frac{1}{|K_1^t|^2\left(\frac{1}{\gamma_{\text{th}}}-\frac{1}{\text{IRR}_t}\right)}\right)^{m_2} \frac{\mathcal{A}\Gamma(m_1-m_2)}{m_2 2^{1-m_1+m_2}\mathcal{B}^{m_2-m_1}}\,{}_1F_2\left(m_2; m_2+1, m_2-m_1+1; \frac{\mathcal{B}^2}{4}\frac{1}{|K_1^t|^2\left(\frac{1}{\gamma_{\text{th}}}-\frac{1}{\text{IRR}_t}\right)}\right) \end{aligned} \quad (90)$$

Finally, in the case of joint TX/RX IQI, (55) can be readily expressed as

$$P_{\text{out}} = \frac{1}{\Gamma(m_1)\Gamma(m_2)} \times G_{1,3}^{2,1}\left(\frac{\left(|K_1^r|^2+|K_2^r|^2\right)\gamma_{\text{th}}}{\left(\frac{|\xi_{11}|^2}{\gamma_{\text{th}}}-\left(|\xi_{12}|^2+|\xi_{21}|^2\right)\right)\overline{\gamma}}\prod_{i=1}^{2}m_i \,\middle|\, \begin{matrix}1\\ m_1, m_2, 0\end{matrix}\right) \tag{95}$$

which, with the aid of (85) and (88), can be alternatively expressed as (96), shown at the bottom of the page, whereas for the case that $m_1 - m_2 \pm (1/2) \in \mathbb{N}$, it can be further simplified to (97), also shown at the bottom of the page. It is recalled here that when the distance separating the involved vehicles is larger than 5 m, the corresponding line-of-sight (LOS) component tends to disappear, and fading becomes more severe [54]. This also includes double Rayleigh fading conditions [25], [58] and [59], which constitute a special case of the double Nakagami-m for $m_2 = m_1 = 1$.

2) Triple Nakagami-m Channel: In case of triple Nakagami-m fading channels, it immediately follows from (51) that the cdf of γ_{ideal} is given by

$$F_{\gamma_{\text{ideal}}}(\gamma) = \frac{1}{\Gamma(m_1)\Gamma(m_2)\Gamma(m_3)} \times G_{1,4}^{3,1}\left(\frac{\gamma}{\overline{\gamma}}m_1m_2m_3 \,\middle|\, \begin{matrix}-\\ m_1, m_2, m_3, 0\end{matrix}\right). \tag{98}$$

Therefore, in case of TX impaired by IQI, (53) can be expressed as

$$P_{\text{out}} = \frac{1}{\Gamma(m_1)\Gamma(m_2)\Gamma(m_3)} \times G_{1,4}^{3,1}\left(\frac{m_1m_2m_3}{|K_1^t|^2\left(\frac{1}{\gamma_{\text{th}}}-\frac{1}{\text{IRR}_t}\right)\overline{\gamma}} \,\middle|\, \begin{matrix}-\\ m_1, m_2, m_3, 0\end{matrix}\right) \tag{99}$$

whereas in the case of RX impaired by IQI, (54) can be rewritten as follows:

$$P_{\text{out}} = \frac{1}{\Gamma(m_1)\Gamma(m_2)\Gamma(m_3)} \times G_{1,4}^{3,1}\left(\frac{1+\frac{1}{\text{IRR}_r}}{\left(\frac{1}{\gamma_{\text{th}}}-\frac{1}{\text{IRR}_r}\right)\overline{\gamma}}m_1m_2m_3 \,\middle|\, \begin{matrix}-\\ m_1, m_2, m_3, 0\end{matrix}\right). \tag{100}$$

Likewise, in the case of joint TX/RX IQI and with the aid of (55), (101), shown at the bottom of the page, immediately follows.

B. Multicarrier V2V Communication System

Here, we assume that $h(k)$ and $h(-k)$ represent the baseband equivalent wireless communication links complex fading coefficients of the kth and $-k$th carriers, respectively, whose magnitudes $|h(k)|$ and $|h(-k)|$ follow a cascaded Nakagami-m distribution. This corresponds to the case of the product of statistically independent but not necessarily identically distributed N^* Nakagami-m random variables. To this effect, it immediately follows that

$$|h(k)| = \prod_{i=1}^{N}|h_i(k)| \tag{102}$$

and

$$|h(-k)| = \prod_{i=1}^{N}|h_i(-k)|. \tag{103}$$

It is recalled that, due to the nature of the surrounding environment, $|h(k)|$ and $|h(-k)|$ can be also adequately modeled by double or triple Nakagami-m processes.

$$P_{\text{out}} = \frac{\mathcal{A}\Gamma(m_2-m_1)}{m_1 2^{m_1-m_2}\mathcal{B}^{m_2-m_1}}\left(\frac{|K_1^r|^2+|K_2^r|^2}{\frac{|\xi_{11}|^2}{\gamma_{\text{th}}}-(|\xi_{12}|^2+|\xi_{21}|^2)}\right)^{m_1} {}_1F_2\left(m_1; m_1+1, m_1-m_2+1; \frac{\mathcal{B}^2}{4}\frac{|K_1^r|^2+|K_2^r|^2}{\frac{|\xi_{11}|^2}{\gamma_{\text{th}}}-(|\xi_{12}|^2+|\xi_{21}|^2)}\right) + \frac{\mathcal{A}\Gamma(m_1-m_2)}{m_2 2^{1-m_1+m_2}\mathcal{B}^{m_2-m_1}}\left(\frac{|K_1^r|^2+|K_2^r|^2}{\frac{|\xi_{11}|^2}{\gamma_{\text{th}}}-(|\xi_{12}|^2+|\xi_{21}|^2)}\right)^{m_2} {}_1F_2\left(m_2; m_2+1, m_2-m_1+1; \frac{\mathcal{B}^2}{4}\frac{|K_1^r|^2+|K_2^r|^2}{\frac{|\xi_{11}|^2}{\gamma_{\text{th}}}-(|\xi_{12}|^2+|\xi_{21}|^2)}\right) \tag{96}$$

$$P_{\text{out}} = \mathcal{A}\sqrt{\pi}\sum_{l=0}^{m_1-m_2-\frac{1}{2}}\frac{\Gamma\left(m_1-m_2+l+\frac{1}{2}\right)\gamma\left(m_1-m_2+l+\frac{1}{2}, \mathcal{B}\sqrt{\frac{|K_1^r|^2+|K_2^r|^2}{\frac{|\xi_{11}|^2}{\gamma_{\text{th}}}-(|\xi_{12}|^2+|\xi_{21}|^2)}}\right)}{l!2^{l-\frac{1}{2}}\mathcal{B}^{m_1+m_2}\Gamma\left(m_1-m_2-l+\frac{1}{2}\right)} \tag{97}$$

$$P_{\text{out}} = \frac{1}{\prod_{i=1}^{3}\Gamma(m_i)}G_{1,4}^{3,1}\left(\frac{|K_1^r|^2+|K_2^r|^2}{\left(\frac{|\xi_{11}|^2}{\gamma_{\text{th}}}-(|\xi_{12}|^2+|\xi_{21}|^2)\right)\overline{\gamma}}m_1m_2m_3 \,\middle|\, \begin{matrix}-\\ m_1, m_2, m_3, 0\end{matrix}\right) \tag{101}$$

1) Double Nakagami-m Channels: In the case of double Nakagami-m fading channels, the SNR CDF is given by (85). Thus, in the case of TX impaired by IQI, (58) is expressed as (104), shown at the bottom of the page. Note that (104) is valid when $m_1 \neq m_2$. For the special case that $m_1 - m_2 \pm \frac{1}{2} \in \mathbb{N}$, the OP can be alternatively expressed with the aid of (88), which yields (105), shown at the bottom of the page.

In the same context, in the case of only RX impaired with IQI, (69) can be rewritten as (106), shown at the bottom of the page, whereas for the case of joint IQI, (79) can be expressed as (107), shown at the bottom of the page. It is again recalled that as the distance between the communicating vehicles becomes larger than 5 m, the involved LOS component tends to disappear, which renders the corresponding fading environments more severe, including double Rayleigh fading conditions, i.e., $(m_2 = m_1 = 1)$.

2) Triple Nakagami-m Channels: In case of triple Nakagami-m channels, the OP in the case that the TX is impaired with IQI is given by (58), namely, (108), shown at the bottom of the next page, whereas in the case of RX impaired with IQI, (69) can be rewritten as (109), shown at the bottom of the next page. Finally, in the case of joint TX/RX IQI, (79) can be expressed as (110), shown at the bottom of the next page. To the best of the authors' knowledge, the derived expressions for the given special cases of N^* Nakagami-m distribution have not been previously reported in the open technical literature.

$$
\begin{aligned}
P_{\text{out}} = q \Bigg\{ & \left(\frac{1}{|K_1^t|^2 \left(\frac{1}{\gamma_{\text{th}}} - \frac{1}{\text{IRR}_t} \right)} \right)^{m_1} \frac{\mathcal{A}\Gamma(m_2 - m_1)}{m_1 2^{m_1 - m_2} \mathcal{B}^{m_2 - m_1}} \, {}_1F_2 \left(m_1; m_1 + 1, m_1 - m_2 + 1; \frac{\mathcal{B}^2}{4} \frac{1}{|K_1^t|^2 \left(\frac{1}{\gamma_{\text{th}}} - \frac{1}{\text{IRR}_t} \right)} \right) \\
& + \left(\frac{1}{|K_1^t|^2 \left(\frac{1}{\gamma_{\text{th}}} - \frac{1}{\text{IRR}_t} \right)} \right)^{m_2} \frac{\mathcal{A}\Gamma(m_1 - m_2)}{m_2 2^{1 - m_1 + m_2} \mathcal{B}^{m_2 - m_1}} \, {}_1F_2 \left(m_2; m_2 + 1, m_2 - m_1 + 1; \frac{\mathcal{B}^2}{4} \frac{1}{|K_1^t|^2 \left(\frac{1}{\gamma_{\text{th}}} - \frac{1}{\text{IRR}_t} \right)} \right) \Bigg\} \\
& + (1 - q) \Bigg\{ \left(\frac{\gamma_{\text{th}}}{|K_1^t|^2} \right)^{m_1} \frac{\mathcal{A}\Gamma(m_2 - m_1)}{m_1 2^{m_1 - m_2} \mathcal{B}^{m_2 - m_1}} \, {}_1F_2 \left(m_1; m_1 + 1, m_1 - m_2 + 1; \frac{\mathcal{B}^2}{4} \frac{\gamma_{\text{th}}}{|K_1^t|^2} \right) \\
& \quad + \left(\frac{\gamma_{\text{th}}}{|K_1^t|^2} \right)^{m_2} \frac{\mathcal{A}\Gamma(m_1 - m_2)}{m_2 2^{1 - m_1 + m_2} \mathcal{B}^{m_2 - m_1}} \, {}_1F_2 \left(m_2; m_2 + 1, m_2 - m_1 + 1; \frac{\mathcal{B}^2}{4} \frac{\gamma_{\text{th}}}{|K_1^t|^2} \right) \Bigg\}
\end{aligned} \tag{104}
$$

$$
\begin{aligned}
P_{\text{out}} = & \sum_{l=0}^{m_1 - m_2 - \frac{1}{2}} \frac{\mathcal{A} q \sqrt{\pi} \Gamma\left(m_1 - m_2 + l + \frac{1}{2} \right)}{l! 2^{l - \frac{1}{2}} \mathcal{B}^{m_1 + m_2} \Gamma\left(m_1 - m_2 - l + \frac{1}{2} \right)} \gamma \left(m_1 - m_2 + l + \frac{1}{2}, \frac{\mathcal{B}}{|K_1^t| \sqrt{\left(\frac{1}{\gamma_{\text{th}}} - \frac{1}{\text{IRR}_t} \right)}} \right) \\
& - \sum_{l=0}^{m_1 - m_2 - \frac{1}{2}} \frac{\mathcal{A}(1 - q) \sqrt{\pi} \Gamma\left(m_1 - m_2 + l + \frac{1}{2} \right)}{l! 2^{l - \frac{1}{2}} \mathcal{B}^{m_1 + m_2} \Gamma\left(m_1 - m_2 - l + \frac{1}{2} \right)} \gamma \left(m_1 - m_2 + l + \frac{1}{2}, \frac{\mathcal{B} \sqrt{\gamma_{\text{th}}}}{|K_1^t|} \right)
\end{aligned} \tag{105}
$$

$$
\begin{aligned}
P_{\text{out}} = q \sum_{k=0}^{p} \frac{(-1)^k \gamma_{\text{th}}^k}{k! \overline{\gamma}^k} \left(1 + \frac{1}{\text{IRR}_r} \right)^k \left(\prod_{i=1}^{2} m_i \right)^k G_{4,4}^{3,3} \left(\frac{\text{IRR}_r}{\gamma_{\text{th}}} \middle| \begin{matrix} 1, k - m_1 + 1, k - m_2 + 1, \ldots, k - m_N + 1, k + 1 \\ m_1, m_2, k, k + 1, 0 \end{matrix} \right) \\
+ (1 - q) \frac{1}{\prod_{i=1}^{2} \Gamma(m_i)} G_{1,3}^{2,1} \left(\frac{\left(1 + \frac{1}{\text{IRR}_r} \right) \gamma_{\text{th}}}{\overline{\gamma}} \prod_{i=1}^{2} m_i \middle| \begin{matrix} 1 \\ m_1, m_2, 0 \end{matrix} \right)
\end{aligned} \tag{106}
$$

$$
\begin{aligned}
P_{\text{out}} = q \sum_{k=0}^{p} \frac{(-1)^k \gamma_{\text{th}}^k \left(|K_1^r|^2 + |K_2^r|^2 \right)^k}{k! \overline{\gamma}^k \left(|\xi_{11}|^2 - \gamma_{\text{th}} |\xi_{12}|^2 \right)^k} \left(\prod_{i=1}^{2} \Gamma(m_i) \right)^k G_{4,4}^{3,3} \left(\frac{|\xi_{11}|^2 - \gamma_{\text{th}} |\xi_{12}|^2}{|\xi_{21}|^2 \gamma_{\text{th}}} \middle| \begin{matrix} 1, k - m_1 + 1, k - m_2 + 1, k + 1 \\ m_1, m_2, k, k + 1, 0 \end{matrix} \right) \\
+ (1 - q) \frac{1}{\prod_{i=1}^{2} \Gamma(m_i)} G_{1,3}^{2,1} \left(\frac{|K_1^r|^2 + |K_2^r|^2}{|\xi_{11}|^2 \overline{\gamma}} \gamma_{\text{th}} \prod_{i=1}^{2} m_i \middle| \begin{matrix} 1 \\ m_1, m_2, 0 \end{matrix} \right)
\end{aligned} \tag{107}
$$

V. Numerical Results

Here, we evaluate and illustrate the effects of IQI on the performance of wireless communications over cascaded Nakagami-m fading channels in terms of the corresponding OP. The notation $m = \{m_1, m_2, \ldots, m_N\}$ denotes up to N^* Nakagami-m channels, i.e., $m = \{m_1, m_2, m_3\}$ for $N = 3$, with fading $m-$parameters of m_1, m_2, and m_3, respectively. We also consider that the SNR is normalized with respect to $\gamma_{\rm th}$, which implies that the OP is evaluated as a function of $\gamma/\gamma_{\rm th}$. Furthermore, it is important to note that, unless otherwise is stated, in the following figures, the numerical results are shown with continuous lines, whereas markers are employed to illustrate the simulation results.

To this end, Fig. 1 shows the OP versus the normalized SNR for the different considered TX/RX scenarios for the case of single-carrier communications. Specifically, we compare the OP between the ideal RF front-end, the RX imbalanced, the TX imbalanced, and joint TX/RX imbalanced cases when the IRR = 20 dB and $\phi = 3^\circ$. We consider the two cases of $\epsilon < 1$ (continuous lines) and $\epsilon > 1$ (dashed lines). Furthermore, different channels have been considered, where $m = 1$, $m = \{1, 1\}$, and $m = \{1, 1, 1, 1\}$ corresponds to the Rayleigh, double Rayleigh, and N^* Rayleigh with $N = 4$ channels, respectively. It is shown that the performance degradation created by the IQI is somewhat less severe compared with the detrimental effects of cascaded fading. For example, for the case of $\gamma/\gamma_{\rm th} =$ 10 dB, the OP in the case of Rayleigh fading is nearly half the OP value in the case of double Rayleigh fading. In addition, in the case of double Rayleigh fading channels, the assumption of an ideal RF front-end results to around 20% error in the corresponding OP. These results highlight the importance of both accurate channel characterization and modeling and accounting for RF impairments in the realistic performance analysis and design of wireless communication systems. It is also interesting to note that when $\epsilon < 1$, the effects of TX IQI only on the OP degradation are more severe than the corresponding effects of RX IQI only. The underlying reason is that the SINR is higher

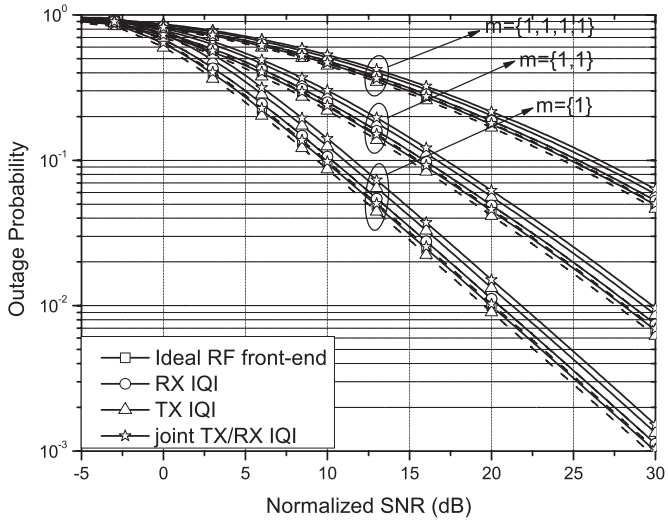

Fig. 1. Single-carrier system $P_{\rm out}$ as a function of the normalized outage SNR when IRR = 20 dB, $\phi = 3^\circ$, $\epsilon \simeq 0.824$ (continuous lines), and $\epsilon \simeq 1.21364$ (dashed lines).

$$P_{\rm out} = \frac{qG_{1,4}^{3,1}\left(\frac{1}{|K_1^t|^2\left(\frac{1}{\gamma_{\rm th}}-\frac{1}{{\rm IRR}_t}\right)\overline{\gamma}}\prod_{i=1}^{3} m_i \,\middle|\, \begin{matrix} 1 \\ m_1, m_2, m_3, 0 \end{matrix}\right)}{\prod_{i=1}^{3}\Gamma(m_i)} + \frac{(1-q)G_{1,4}^{3,1}\left(\frac{\gamma_{\rm th}}{|K_1^t|^2\overline{\gamma}}\prod_{i=1}^{3} m_i \,\middle|\, \begin{matrix} 1 \\ m_1, m_2, m_3, 0 \end{matrix}\right)}{\prod_{i=1}^{3}\Gamma(m_i)} \tag{108}$$

$$P_{\rm out} = q\sum_{k=0}^{p}\frac{(-1)^k\gamma_{\rm th}^k}{k!\overline{\gamma}^k}\left(1+\frac{1}{{\rm IRR}_r}\right)^k\left(\prod_{i=1}^{3} m_i\right)^k G_{5,5}^{4,4}\left(\frac{{\rm IRR}_t}{\gamma_{\rm th}} \,\middle|\, \begin{matrix} 1, k-m_1+1, k-m_2+1, k-m_3+1, k+1 \\ m_1, m_2, m_3, k, k+1, 0 \end{matrix}\right) + (1-q)\frac{1}{\prod_{i=1}^{3}\Gamma(m_i)}G_{1,4}^{3,1}\left(\frac{\left(1+\frac{1}{{\rm IRR}_r}\right)\gamma_{\rm th}}{\overline{\gamma}}\prod_{i=1}^{3} m_i \,\middle|\, \begin{matrix} 1 \\ m_1, m_2, m_3, 0 \end{matrix}\right) \tag{109}$$

$$P_{\rm out} = q\sum_{k=0}^{p}\frac{(-1)^k\gamma_{\rm th}^k\left(|K_1^r|^2+|K_2^r|^2\right)^k}{k!\overline{\gamma}^k\left(|\xi_{11}|^2-\gamma_{\rm th}|\xi_{12}|^2\right)^k}\left(\prod_{i=1}^{3}\Gamma(m_i)\right)^k \times G_{5,5}^{4,4}\left(\frac{|\xi_{11}|^2-\gamma_{\rm th}|\xi_{12}|^2}{|\xi_{21}|^2\gamma_{\rm th}} \,\middle|\, \begin{matrix} 1, k-m_1+1, k-m_2+1, k-m_3+1, k+1 \\ m_1, m_2, m_3, k, k+1, 0 \end{matrix}\right) + (1-q)\frac{1}{\prod_{i=1}^{3}\Gamma(m_i)}G_{1,4}^{3,1}\left(\frac{|K_1^r|^2+|K_2^r|^2}{|\xi_{11}|^2\overline{\gamma}}\gamma_{\rm th}\prod_{i=1}^{3} m_i \,\middle|\, \begin{matrix} 1 \\ m_1, m_2, m_3, 0 \end{matrix}\right) \tag{110}$$

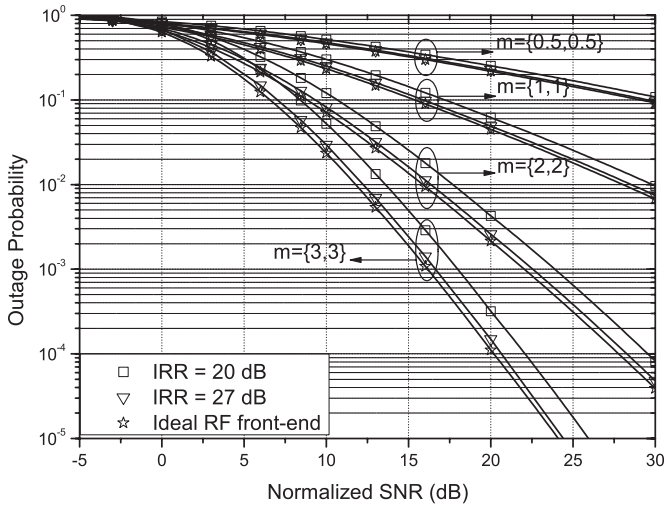

Fig. 2. Single-carrier system $P_{\rm out}$ as a function of the normalized outage SNR, for different values of IRR, when $\epsilon < 1$, and $\phi = 3^\circ$.

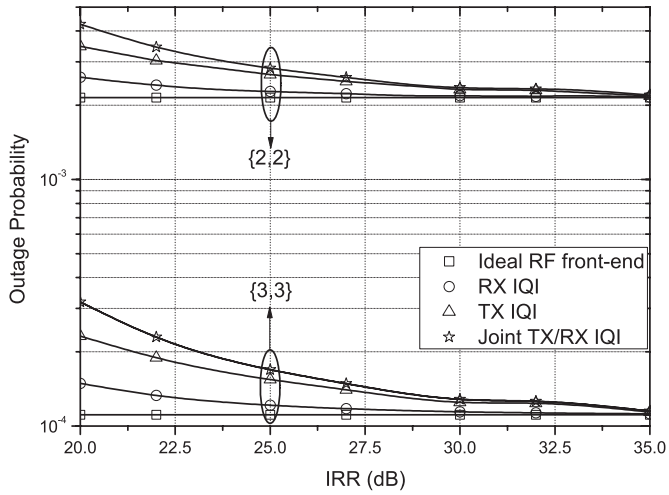

Fig. 3. Single-carrier system $P_{\rm out}$ as a function of the IRR when SNR $=$ 20 dB and $\phi = 3^\circ$.

in the case of RX IQI only than in the case of TX IQI only since the noise is multiplied by $(|K_1^r|^2 + |K_2^r|^2)$, which, for $\epsilon < 1$, does not exceed 1. Moreover, it is worth mentioning that in the case of $\epsilon > 1$, the RX IQI effects are the most severe since the noise is multiplied by $(|K_1^r|^2 + |K_2^r|^2)$, which, in this case, is greater than 1. Interestingly, in case of $\epsilon > 1$, the TX IQI only system outperforms even the corresponding ideal RF front-end system. As can be drawn from (8) and (9), when $\epsilon > 1$, for practical levels of IQI, it follows that $|K_1^t|^2 > 1$, and $|K_2^t|^2 \to 0$. Therefore, (15) can be tightly approximated as

$$\gamma \approx |K_1^t|^2 \gamma_{\rm ideal} \tag{111}$$

which, for $\epsilon > 1$, is greater than $\gamma_{\rm ideal}$.

Fig. 2 shows the effects of the IRR on the OP in case of single-carrier communication systems considering double Rayleigh and double Nakagami-m, with $m = \{0.5, 0.5\}$, $m = \{2, 2\}$, and $m = \{3, 3\}$ fading conditions with joint TX/RX IQI. It is evident that the OP decreases as the m values are increased, for a given SNR value, whereas as expected, the OP is improved when the IRR is increased. For example, for the case of double Nakagami-m conditions with $\overline{\gamma} = 10$ dB, taking an RF front end with an IRR of 27 dB instead of 20 dB, decreases the corresponding OP by 30%. Notably, since the IRR of practical RF front ends lies in the range of 20–40 dB, these results highlight the importance of taking RF impairments such as the IQI into consideration. Likewise, it is also shown that it is of paramount importance to take into account the effects of cascaded fading conditions as the difference in comparison with nonmultiplicative fading is about an order of magnitude in both low- and high-SNR regimes.

Fig. 3 shows the effects of the IRR on the OP for the different considered TX/RX scenarios assuming double Nakagami-m, with $m = \{2, 2\}$ and $m = \{3, 3\}$, fading channels. It is evident that the OP is lower for the case of double Nakagami-m fading with $m = \{3, 3\}$ compared with the double Nakagami-m fading with $m = \{2, 2\}$, whereas, as expected, the OP is improved when the IRR is increased. For example, for the case of double Nakagami-m with $m = \{3, 3\}$ conditions with $\gamma/\gamma_{\rm th} = 20$ dB, taking an RF front end with an IRR of 25 dB instead of 20 dB, decreases the corresponding OP by 47%, in the case of joint TX/RX IQI. Consequently, for realistic levels of hardware imperfections, these results highlight the detrimental effects of IQI and indicate the importance of taking RF impairments and the statistics of the channel into consideration.

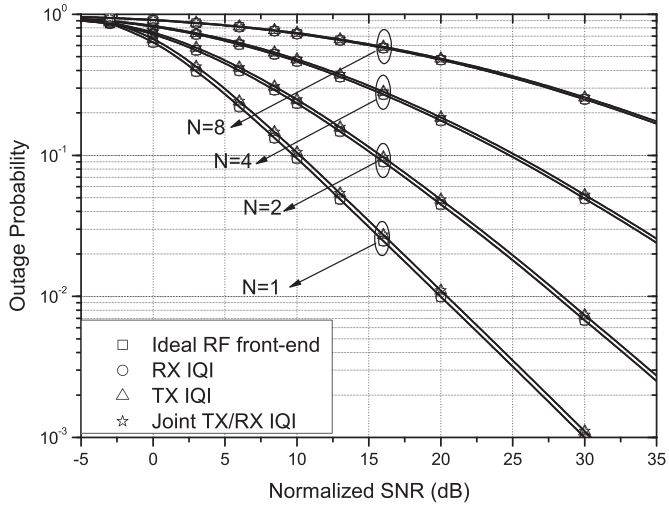

Fig. 4. Multicarrier system $P_{\rm out}$ as a function of the normalized outage SNR when $q = 0$, IRR $= 25$ dB, and $\phi = 3^\circ$, considering N^* Rayleigh channels.

Next, we consider the case of multicarrier transmission and evaluate the effects of IQI on the OP in the case of signal absence and signal presence at the carrier $-k$, i.e., $q = 0$ and $q = 1$, respectively. We assume mutually uncorrelated channel gains between the carrier k and its image $-k$. The OP of multicarrier systems with $q = 0$ over N^* Rayleigh channels is demonstrated in Fig. 4, where the impact of cascaded channels on the corresponding performance is clearly observed. Yet, it is noticed that when there is no signal in the image carrier, the signal carried by the carrier k is interference free. As a result, the performance degradation caused by the RF front-end IQI is

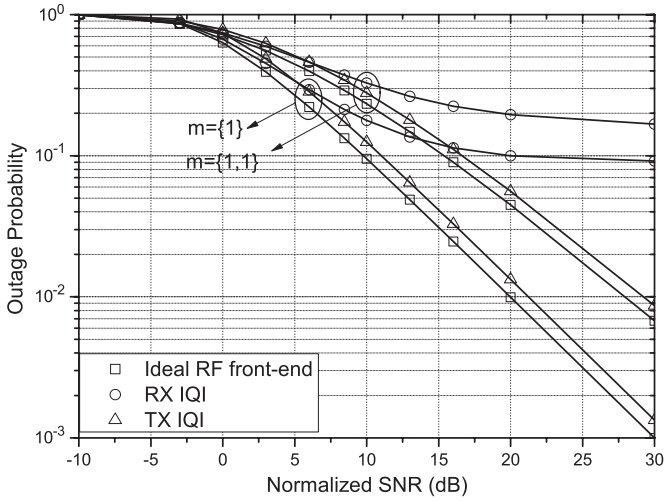

Fig. 5. Multicarrier system P_{out} as a function of the normalized outage SNR when $q = 1$, IRR $= 20$ dB, and $\phi = 3^\circ$.

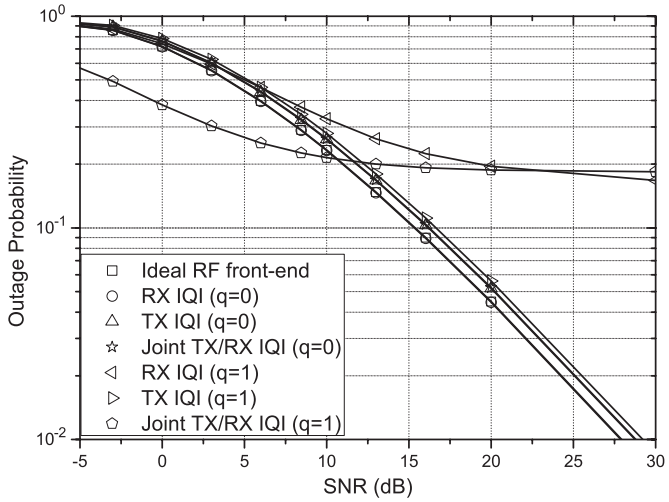

Fig. 6. Multicarrier system P_{out} as a function of the normalized outage SNR when $m = \{1, 1\}$, IRR $= 20$ dB, and $\phi = 3^\circ$.

much lower than the corresponding degradation in the single-carrier transmission scenario. In fact, when IRR $= 25$ dB, the OP is nearly the same as in the cases that the TX and/or RX are ideal. These results are expected since the mirror-interference effects of IQI are nullified when there is no signal in the carrier $-k$. Furthermore, we observe that as N increases, the performance degradation become more severe. For instance, for $N = 8$, the OP is higher than 10^{-1}, even for extreme values of normalized SNR. This finding reveals that in the case of $q = 0$, the main source of OP degradation is the impact of the cascaded channels and not the hardware imperfections.

Fig. 5 shows the OP versus the normalized SNR for multicarrier systems, over both Rayleigh and double Rayleigh channels, for the case of a signal present in the carrier $-k$, i.e., $q = 1$. In this case, the IQI causes distortion of the transmitted baseband equivalent signal at the kth carrier, $s(k)$, by its image signal at the carrier $-k$. Furthermore, we observe a lower bound in the case of ideal TX and I/Q imbalanced RX. Intuitively, in the case of TX IQI only, mirroring occurs already at TX and the total signal at carrier k, original and mirrored term, both travel through $h(k)$, i.e., fading does not change their ratio. However, in the case of RX IQI only, mirroring occurs after wireless transmission over the multiplicative fading channel; therefore, there can be a challenging scenario when $h(k)$ has low value (deep fade) and $h(-k)$ is strong. Thus, the mirrored term can be very strong. Furthermore, as can be drawn from (41), in the high SNR regime, in the presence of signal in the carrier $-k$, the instantaneous SINR per symbol can be accurately approximated by

$$\gamma(k) \approx \frac{\gamma_{\text{ideal}}(k)}{\gamma_{\text{ideal}}(-k)} \text{IRR}_r. \tag{112}$$

Assuming $\gamma_{\text{ideal}}(k) \approx \gamma_{\text{ideal}}(-k)$, it follows that

$$\gamma(k) \approx \text{IRR}_r. \tag{113}$$

In other words, we observe that the maximum achievable SINR is constrained to the IRR levels because of the effects of IQI.

To this effect, it is shown that the SINR exhibits an upper bound, which in turn results to a lower bound in the corresponding OP performance. It is noted that the same behavior is experienced in the case of joint TX/RX IQI. Hence, it is evident that this lower bound can create detrimental effects on the performance of communication systems, which stresses the importance of the provided performance analysis and the requirement for efficient compensation techniques.

Finally, Fig. 6 compares the OP of multicarrier systems over double Rayleigh channels, when $q = 0$ and $q = 1$. It is observed that the detrimental effects of IQI on the OP performance are significantly increased when a signal is present in the carrier $-k$. Specifically, in the case of $q = 1$ and RX or joint TX/RX IQI, as SNR increases, the mirror interference increases, resulting to an OP lower bound. In the worst-case scenario, where IRR $= 20$ dB, this bound is on the order of 9×10^{-1}, which may not be acceptable in practice. Meanwhile, the presence of a signal in the carrier $-k$ creates no impact, as expected, on the performance of multicarrier systems, when the RF front end is considered ideal.

VI. Conclusion

This paper has investigated the OP performance of single-carrier and multicarrier systems over cascaded Nakagami-m channels in the presence of IQI at the RF front end. For the multicarrier systems, we considered the case in which the channel $-k$ is both occupied and unoccupied by an information signal, whereas for each system, we considered three scenarios in our analysis corresponding to ideal TX with I/Q imbalanced RX, I/Q imbalanced TX with ideal RX, and joint I/Q imbalanced TX and RX. The ideal case was also taken into consideration for comparison and the derived analytic results were validated through extensive comparisons with respective results from computer simulations. It was shown that, in single-carrier systems, the performance degradation caused by IQI in one or both of the RF front ends is more significant than in multicarrier systems when $q = 0$. However, the most challenging case, by

far, is when $q = 1$ in the multicarrier system, particularly in the case of RX or joint TX/RX IQI. Furthermore, it was observed in all cases that IQI introduces significant effects that result in nonnegligible OP degradations, whereas a lower bound on the OP was observed in the high-SNR regime. Additionally, it was shown that the effect of cascaded fading conditions on the OP performance are significant as the number of scatterers along with the involved severity of fading can increase or decrease the corresponding performance by about an order of magnitude at both the low and high SNR regimes. Finally, the validity and practical usefulness of the offered results were verified by applying them in realistic wireless applications in the context of V2V communications over cascaded fading channels providing meaningful insights on the performance of such systems.

ACKNOWLEDGMENT

The authors would like to thank the editor and the anonymous reviewers for their constructive comments and criticism.

REFERENCES

[1] A. Abidi, "Direct-conversion radio transceivers for digital communications," *IEEE J. Solid-State Circuits*, vol. 30, no. 12, pp. 1399–1410, Dec. 1995.

[2] S. Mirabbasi and K. Martin, "Classical and modern receiver architectures," *IEEE Commun. Mag.*, vol. 38, no. 11, pp. 132–139, Nov. 2000.

[3] M. Valkama, M. Renfors, and V. Koivunen, "Advanced methods for I/Q imbalance compensation in communication receivers," *IEEE Trans. Signal Process.*, vol. 49, no. 10, pp. 2335–2344, Oct. 2001.

[4] B. Razavi, *RF Microelectronics*, vol. 1. Englewood Cliffs, NJ, USA: Prentice-Hall, 1998.

[5] T. Schenk, *RF Imperfections in High-Rate Wireless Systems*. Dordrecht, The Netherlands: Springer-Verlag, 2008.

[6] T. T. Duy, T. Duong, D. Benevides da Costa, V. N. Q. Bao, and M. Elkashlan, "Proactive relay selection with joint impact of hardware impairment and co-channel interference," *IEEE Trans. Commun.*, vol. 63, no. 5, pp. 1594–1606, May 2015.

[7] P. Rykaczewski, M. Valkama, and M. Renfors, "On the connection of I/Q imbalance and channel equalization in direct-conversion transceivers," *IEEE Trans. Veh. Technol.*, vol. 57, no. 3, pp. 1630–1636, May 2008.

[8] A. Gokceoglu *et al.*, "Mutual information analysis of OFDM radio link under phase noise, IQ imbalance and frequency-selective fading channel," *IEEE Trans. Wireless Commun.*, vol. 12, no. 6, pp. 3048–3059, Jun. 2013.

[9] A. ElSamadouny, A. Gomaa, and N. Al-Dhahir, "Likelihood-based spectrum sensing of OFDM signals in the presence of Tx/Rx I/Q imbalance," in *Proc. IEEE Global Commun. Conf.*, Dec. 2012, pp. 3616–3621.

[10] M. Mokhtar, A.-A. A. Boulogeorgos, G. K. Karagiannidis, and N. Al-Dhahir, "Dual-Hop OFDM opportunistic AF relaying under joint transmit/receive I/Q imbalance," in *Proc. IEEE Global Telecommun. Conf.*, Atlanta, GA, USA, Dec. 2013, pp. 4287–4292.

[11] A. Abdi and M. Kaveh, "K distribution: An appropriate substitute for Rayleigh-lognormal distribution in fading-shadowing wireless channels," *Electron. Lett.*, vol. 34, no. 9, pp. 851–852, Apr. 1998.

[12] P. Bithas, N. Sagias, P. Mathiopoulos, G. Karagiannidis, and A. Rontogiannis, "On the performance analysis of digital communications over generalized-K fading channels," *IEEE Commun. Lett.*, vol. 10, no. 5, pp. 353–355, May 2006.

[13] A. Laourine, M.-S. Alouini, S. Affes, and A. Stephenne, "On the performance analysis of composite multipath/shadowing channels using the G-distribution," *IEEE Trans. Commun.*, vol. 57, no. 4, pp. 1162–1170, Apr. 2009.

[14] P. Bithas, "Weibull-gamma composite distribution: Alternative multipath/shadowing fading model," *Electron. Lett.*, vol. 45, no. 14, pp. 749–751, Jul. 2009.

[15] C. Zhong, M. Matthaiou, G. Karagiannidis, A. Huang, and Z. Zhang, "Capacity bounds for AF dual-hop relaying in cal G fading channels," *IEEE Trans. Veh. Technol.*, vol. 61, no. 4, pp. 1730–1740, May 2012.

[16] P. C. Sofotasios, T. Tsiftsis, M. Ghogho, L. Wilhelmsson, and M. Valkama, "The $\eta - \mu$/IG distribution: A novel physical multipath/shadowing fading model," in *Proc. IEEE ICC*, Jun. 2013, pp. 5715–5719.

[17] P. Bithas, N. Sagias, and P. Mathiopoulos, "The bivariate generalized-(g) distribution and its application to diversity receivers," *IEEE Trans. Commun.*, vol. 57, no. 9, pp. 2655–2662, Sep. 2009.

[18] J. Zhang, M. Matthaiou, Z. Tan, and H. Wang, "Performance analysis of digital communication systems over composite $\eta - \mu$/gamma fading channels," *IEEE Trans. Veh. Technol.*, vol. 61, no. 7, pp. 3114–3124, Sep. 2012.

[19] J. F. Paris, "Advances in the statistical characterization of fading: From 2005 to present," *Int. J. Antennas Propag.*, vol. 2014, pp. 1–5, 2014.

[20] P. C. Sofotasios *et al.*, "The $\kappa - \mu$/inverse-gaussian composite statistical distribution in RF and FSO wireless channels," in *Proc. IEEE 78th VTC—Fall*, Sep. 2013, pp. 1–5.

[21] J. Paris, "Statistical characterization of $\kappa - \mu$ shadowed fading," *IEEE Trans. Veh. Technol.*, vol. 63, no. 2, pp. 518–526, Feb. 2014.

[22] J. B. Andersen, "Statistical distributions in mobile communications using multiple scattering," in *Proc. 27th URSI Gen. Assem.*, 2002, pp. 1–25.

[23] G. K. Karagiannidis, N. C. Sagias, and P. T. Mathiopoulos, "N*Nakagami: A novel stochastic model for cascaded fading channels," *IEEE Trans. Commun.*, vol. 55, no. 8, pp. 1453–1458, Aug. 2007.

[24] P. C. Sofotasios, L. Mohjazi, S. Muhaidat, M. Al-Qutayri, and G. Karagiannidis, "Energy detection of unknown signals over cascaded fading channels," *IEEE Antennas Wireless Propag. Lett.*, to be published.

[25] V. Erceg, S. J. Fortune, J. Ling, A. Rustako, and R. A. Valenzuela, "Comparisons of a computer-based propagation prediction tool with experimental data collected in urban microcellular environments," *IEEE J. Sel. Areas Commun.*, vol. 15, no. 4, pp. 677–684, May 1997.

[26] C. Studer, M. Wenk, and A. Burg, "MIMO transmission with residual transmit-RF impairments," in *Proc. Int. ITG Workshop Smart Antennas*, Bremen, Germany, Feb. 2010, pp. 189–196.

[27] E. Bjornson, P. Zetterberg, and M. Bengtsson, "Optimal coordinated beamforming in the multicell downlink with transceiver impairments," in *Proc. IEEE Global Communications Conf.*, Anaheim, CA, USA, Dec. 2012, pp. 4775–4780.

[28] E. Bjornson, A. Papadogiannis, M. Matthaiou, and M. Debbah, "On the impact of transceiver impairments on AF relaying," in *Proc. IEEE Int. Conf. Acoust., Speech Signal Process.*, Vancouver, BC, Canada, May 2013, pp. 4948–4952.

[29] E. Bjornson, P. Zetterberg, M. Bengtsson, and B. Ottersten, "Capacity limits and multiplexing gains of MIMO channels with transceiver impairments," *IEEE Commun. Lett.*, vol. 17, no. 1, pp. 91–94, Jan. 2013.

[30] E. Bjornson, M. Matthaiou, and M. Debbah, "A new look at dual-hop relaying: Performance limits with hardware impairments," *IEEE Trans. Commun.*, vol. 61, no. 11, pp. 4512–4525, Nov. 2013.

[31] A.-A. A. Boulogeorgos, N. Chatzidiamantis, G. K. Karagiannidis, and L. Georgiadis, "Energy detection under RF impairments for cognitive radio," in *Proc. IEEE ICC—CoCoNet*, London, U.K., Jun. 2015, pp. 955–960.

[32] A.-A. A. Boulogeorgos, N. D. Chatzidiamantis, and G. K. Karagiannidis, "Spectrum sensing under hardware constraints," to be published. [Online]. Available: http://arxiv.org/abs/1510.06527

[33] O. Ozgur, R. Hamila, and N. Al-Dhahir, "Exact average OFDM subcarrier SINR analysis under joint transmit-receive I/Q imbalance," *IEEE Trans. Veh. Technol.*, vol. 63, no. 8, pp. 4125–4130, Oct. 2014.

[34] C.-L. Liu, "Impacts of I/Q imbalance on QPSK-OFDM-QAM detection," *IEEE Trans. Consum. Electron.*, vol. 44, no. 3, pp. 984–989, Aug. 1998.

[35] A. Tarighat, R. Bagheri, and A. Sayed, "Compensation schemes and performance analysis of IQ imbalances in OFDM receivers," *IEEE Trans. Signal Process.*, vol. 53, no. 8, pp. 3257–3268, Aug. 2005.

[36] J. Qi, S. Aïssa, and M.-S. Alouini, "Analysis and compensation of I/Q imbalance in amplify-and-forward cooperative systems," in *Proc. IEEE Wireless Commun. Netw. Conf.*, Shanghai, China, Apr. 2012, pp. 215–220.

[37] J. Qi, S. Aïssa, and M.-S. Alouini, "Impact of I/Q imbalance on the performance of two-way CSI-assisted AF relaying," in *Proc. IEEE Wireless Commun. Netw. Conf.*, Shanghai, China, Apr. 2013, pp. 2507–2512.

[38] J. Qi, S. Aïssa, and M.-S. Alouini, "Dual-hop amplify-and-forward cooperative relaying in the presence of Tx and Rx in-phase and quadrature-phase imbalance," *IET Commun.*, vol. 8, no. 3, pp. 287–298, Feb. 2014.

[39] J. Li, M. Matthaiou, and T. Svensson, "I/Q imbalance in AF dual-hop relaying: Performance analysis in Nakagami-m fading," *IEEE Trans. Commun.*, vol. 62, no. 3, pp. 836–847, Mar. 2014.

[40] M. Mokhtar, A.-A. A. Boulogeorgos, G. K. Karagiannidis, and N. Al-Dhahir, "OFDM opportunistic relaying under joint transmit/receive I/Q imbalance," *IEEE Trans. Commun.*, vol. 62, no. 5, pp. 1458–1468, May 2014.

[41] J. Li, M. Matthaiou, and T. Svensson, "I/Q imbalance in two-way AF relaying," *IEEE Trans. Commun.*, vol. 62, no. 7, pp. 2271–2285, Jul. 2014.

[42] J. Li, M. Matthaiou, and T. Svensson, "I/Q imbalance in two-way AF relaying: Performance analysis and detection mode switch," in *Proc. IEEE GLOBECOM*, Dec. 2014, pp. 4001–4007.
[43] J. Qi and S. Aïssa, "Analysis and compensation of I/Q imbalance in MIMO transmit-receive diversity systems," *IEEE Trans. Commun.*, vol. 58, no. 5, pp. 1546–1556, May 2010.
[44] T. C. W. Schenk, E. R. Fledderus, and P. F. M. Smulders, "Performance analysis of zero-if MIMO OFDM transceivers with IQ imbalance," *J. Commun.*, vol. 2, no. 7, pp. 9–19, 2007.
[45] B. Maham, O. Tirkkonen, and A. Hjørungnes, "Impact of transceiver I/Q imbalance on transmit diversity of beamforming OFDM systems," *IEEE Trans. Commun.*, vol. 60, no. 3, pp. 643–648, Mar. 2012.
[46] B. Narasimhan, S. Narayanan, H. Minn, and N. Al-Dhahir, "Reduced-complexity baseband compensation of joint Tx/Rx I/Q imbalance in mobile MIMO-OFDM," *IEEE Trans. Wireless Commun.*, vol. 9, no. 5, pp. 1720–1728, May 2010.
[47] L. Anttila, M. Valkama, and M. Renfors, "Circularity-based I/Q imbalance compensation in wideband direct-conversion receivers," *IEEE Trans. Veh. Commun.*, vol. 57, no. 4, pp. 2099–2113, Jul. 2008.
[48] M. Valkama, J. Pirskanen, and M. Renfors, "Signal processing challenges for applying software radio principles in future wireless terminals: An overview," *Int. J. Commun. Syst.*, vol. 15, no. 8, pp. 741–769, 2002.
[49] A.-A. A. Boulogeorgos, V. M. Kapinas, R. Schober, and G. K. Karagiannidis, "I/Q-imbalance self-interference coordination," vol. 15, no. 6, pp. 4157–4170, Jun. 2016.
[50] A.-A. A. Boulogeorgos, H. Bany Salameh, and G. K. Karagiannidis, "On the effects of I/Q imbalance on sensing performance in full-duplex cognitive radios," in *Proc. IEEE WCNC-IWSS*, Doha, Qatar, Apr. 2016.
[51] S. J. Grant and J. K. Cavers, "Analytical calculation of outage probability for a general cellular mobile radio system," in *Proc. IEEE Veh. Technol. Conf.*, Amsterdam, The Netherlands, 1999, vol. 3, pp. 1372–1376.
[52] I. S. Gradshteyn and I. M. Ryzhik, *Table of Integrals, Series, and Products*, 6th ed. New York, NY, USA: Academic, 2000.
[53] H. Ilhan, M. Uysal, and I. Altunbas, "Cooperative diversity for intervehicular communication: Performance analysis and optimization," *IEEE Trans. Veh. Commun.*, vol. 58, no. 7, pp. 3301–3310, Sep. 2009.
[54] A. Molisch, F. Tufvesson, J. Karedal, and C. Mecklenbrauker, "A survey on vehicle-to-vehicle propagation channels," *IEEE Wireless Commun. Mag.*, vol. 16, no. 6, pp. 12–22, Dec. 2009.
[55] M. Kihl, K. Bur, F. Tufvesson, and J. Aparicio Ojea, "Simulation modelling and analysis of a realistic radio channel model for V2V communications," in *Proc. Int. Congr. Ultra Modern Telecommun. Control Syst. Workshops*, Moscow, Russia, Oct. 2010, pp. 981–988.
[56] M. K. Simon and M.-S. Alouini, *Digital Communication Over Fading Channels*, vol. 95. New York, NY, USA: Wiley, 2005.
[57] A. P. Prudnikov, Y. A. Brychkov, and O. I. Marichev, *Inegrals and Series, Vol. 2: Special Functions*. New York, NY, USA: Gordon and Breach, 1992.
[58] H. Hadizadeh, S. Muhaidat, and I. Bajic, "Impact of imperfect channel estimation on the performance of inter-vehicular cooperative networks," in *Proc. IEEE Biennial Symp. Commun.*, Kingston, ON, Canada, May 2010, pp. 373–376.
[59] M. Shirkhani, Z. Tirkan, and A. Taherpour, "Performance analysis and optimization of two-way cooperative communications in inter-vehicular networks," in *Proc. IEEE Int. Conf. Wireless Commun. Signal Process.*, Huangshan, China, Oct. 2012, pp. 1–6.

Alexandros-Apostolos A. Boulogeorgos (S'11) was born in Trikala, Greece. He received the Diploma (five years) in electrical and computer engineering from Aristotle University of Thessaloniki, Thessaloniki, Greece, in 2012. He is currently working toward the Ph.D. degree with the Department of Electrical and Computer Engineering, Aristotle University of Thessaloniki.

His current research interests include fading channel characterization, cooperative communications, cognitive radio, interference management, and hardware-constrained communications.

Paschalis C. Sofotasios (M'16) was born in Volos, Greece, in 1978. He received the M.Eng. degree from the University of Newcastle upon Tyne, U.K., in 2004; the M.Sc. degree from the University of Surrey, Surrey, U.K., in 2006; and the Ph.D. degree from the University of Leeds, Leeds, U.K., in 2011.

His Master's studies were funded by a scholarship from U.K. Engineering and Physical Sciences Research Council (UK-EPSRC), and his doctoral studies were sponsored by UK-EPSRC and Pace plc. He was a Postdoctoral Researcher with the University of Leeds until August 2013 and a Visiting Researcher with the University of California, Los Angeles, CA, USA; Aristotle University of Thessaloniki, Thessaloniki, Greece; and Tampere University of Technology, Tampere, Finland. Since Fall 2013, he has been a Postdoctoral Research Fellow with the Department of Electronics and Communications Engineering, Tampere University of Technology and with the Wireless Communications Systems Group, Aristotle University of Thessalonski. His research interests include fading channel characterization, cognitive radio, cooperative communications, optical wireless communications, and the theory and properties of special functions and statistical distributions.

Dr. Sofotasios received the 2012 and 2015 Exemplary Reviewer Award from the IEEE COMMUNICATION LETTERS and the IEEE TRANSACTIONS ON COMMUNICATIONS, respectively, and the Best Paper Award at the International Conference on Ubiquitous and Future Networks in 2013.

Bassant Selim (S'15) received the B.Sc. degree in communications engineering from the French University in Egypt, Cairo, Egypt, and the Master's degree in communication systems from Pierre et Marie Curie (Paris XI) University, Paris, France, in 2011. She is currently working toward the Ph.D. degree with Khalifa University, Abu Dhabi, United Arab Emirates.

Her research interests include wireless communications, cognitive radio, spectrum sensing, and radio-frequency impairments.

Sami Muhaidat (S'01–M'07–SM'11) received the Ph.D. degree in electrical and computer engineering from the University of Waterloo, Waterloo, ON, Canada, in 2006.

From 2007 to 2008, he was a Natural Sciences and Engineering Research Council (NSERC) Postdoctoral Fellow with the Department of Electrical and Computer Engineering, University of Toronto, Toronto, ON. From 2008 to 2012, he was an Assistant Professor with the School of Engineering Science, Simon Fraser University, Burnaby, BC, Canada. He is currently an Associate Professor with Khalifa University, Abu Dhabi, United Arab Emirates, and a Visiting Professor with the Department of Electrical and Computer Engineering, University of Western Ontario, London, ON. He is also a Visiting Reader with the Faculty of Engineering, University of Surrey, Surrey, U.K. He is the author of more than 100 journal and conference papers on these topics. His research interests include advanced digital signal processing techniques for communications, cooperative communications, vehicular communications, multiple-input multiple-output, and machine learning.

Dr. Muhaidat currently serves as a Senior Editor for the IEEE COMMUNICATIONS LETTERS, as an Editor for the IEEE TRANSACTIONS ON COMMUNICATIONS, and as an Associate Editor for the IEEE TRANSACTIONS ON VEHICULAR TECHNOLOGY. He received several scholarships during his undergraduate and graduate studies and won the NSERC Postdoctoral Fellowship competition in 2006.

George K. Karagiannidis (M'96–SM'03–F'14) was born in Pythagorion, Samos Island, Greece. He received the University Diploma (5 years) and the Ph.D. degree, both in electrical and computer engineering, from the University of Patras, Patras, Greece, in 1987 and 1999, respectively.

From 2000 to 2004, he was a Senior Researcher with the Institute for Space Applications and Remote Sensing, National Observatory of Athens, Athens, Greece. Since June 2004, he has been with the faculty of Aristotle University of Thessaloniki, Thessaloniki, Greece, where he is currently a Professor with the Department of Electrical and Computer Engineering and the Director of Digital Telecommunications Systems and Networks Laboratory. He is an Honorary Professor with South West Jiaotong University, Chengdu, China. He is the author or coauthor of more than 400 technical papers published in scientific journals and presented at international conferences. He is also the author of the Greek edition of *Telecommunications Systems* and the coauthor of *Advanced Optical Wireless Communications Systems* (Cambridge, 2012). His research interests include digital communications systems with emphasis on wireless communications, optical wireless communications, wireless power transfer and applications, molecular communications, communications and robotics, and wireless security.

Dr. Karagiannidis has served as the General Chair, the Technical Program Chair, and a member of Technical Program Committees of several IEEE and non-IEEE conferences. In the past, he served as an Editor for the IEEE TRANSACTIONS ON COMMUNICATIONS, as a Senior Editor for the IEEE COMMUNICATIONS LETTERS, as an Editor for the *EURASIP Journal of Wireless Communications & Networks*, as well as a Guest Editor for the IEEE JOURNAL ON SELECTED AREAS IN COMMUNICATIONS several times. From 2012 to 2015, he was the Editor-in Chief of IEEE COMMUNICATIONS LETTERS. He was selected as a 2015 Thomson Reuters Highly Cited Researcher.

Mikko Valkama (SM'15) was born in Pirkkala, Finland, on November 27, 1975. He received the M.Sc. and Ph.D. Degrees (both with honors) in electrical engineering from Tampere University of Technology (TUT), Tampere, Finland, in 2000 and 2001, respectively.

In 2003, he was a Visiting Researcher with the Communications Systems and Signal Processing Institute, San Diego State University, San Diego, CA, USA. He is currently a Full Professor and the Department Vice Head with the Department of Electronics and Communications Engineering, TUT. His main research interests include communications signal processing, estimation and detection techniques, signal processing algorithms for software-defined flexible radios, cognitive radio, full-duplex radio, radio localization, fifth-generation mobile cellular radio, digital transmission techniques such as different variants of multicarrier modulation methods and orthogonal frequency-division multiplexing, and radio resource management for *ad hoc* and mobile networks.

Dr. Valkama received the Best Ph.D. Thesis award from the Finnish Academy of Science and Letters for his dissertation entitled "Advanced I/Q Signal Processing for Wideband Receivers: Models and Algorithms" in 2002.